

Density Model for Unidentified Beaked Whales (*Ziphiidae spp.*) for the U.S. East Coast: Supplementary Report

Model Version 7.1

Duke University Marine Geospatial Ecology Laboratory*

2023-05-27


Citation

When citing our methodology or results generally, please cite Roberts et al. (2016, 2023). The complete references appear at the end of this document. We are preparing a new article for a peer-reviewed journal that will eventually replace those. Until that is published, those are the best general citations.

When citing this model specifically, please use this reference:

Roberts JJ, Yack TM, Cañadas A, Fujioka E, Halpin PN, Barco SG, Boisseau O, Chavez-Rosales S, Cole TVN, Cotter MP, Cummings EW, Davis GE, DiGiovanni Jr. RA, Garrison LP, Gowan TA, Jackson KA, Kenney RD, Khan CB, Lockhart GG, Lomac-MacNair KS, McAlarney RJ, McLellan WA, Mullin KD, Nowacek DP, O'Brien O, Pabst DA, Palka DL, Quintana-Rizzo E, Redfern JV, Rickard ME, White M, Whitt AD, Zoidis AM (2022) Density Model for Unidentified Beaked Whales (*Ziphiidae spp.*) for the U.S. East Coast, Version 7.1, 2023-05-27, and Supplementary Report. Marine Geospatial Ecology Laboratory, Duke University, Durham, North Carolina.

Copyright and License

 This document and the accompanying results are © 2023 by the Duke University Marine Geospatial Ecology Laboratory and are licensed under a [Creative Commons Attribution 4.0 International License](https://creativecommons.org/licenses/by/4.0/).

Model Version History

Version	Date	Description
5	2017-06-01	Began update to Roberts et al. (2015) models. Introduced new surveys from AMAPPS, NARWSS, UNCW, VAMSC, and the SEUS NARW teams. Updated modeling methodology. Refitted detection functions. Split Roberts et al. (2015) beaked whale guild into three taxa: Cuvier's beaked whale, the Mesoplodont guild, and unidentified beaked whales. Fit new spatial models from scratch using new and reprocessed covariates.
6	2017-08-10	Removed biological predictors, reintroduced pre-1998 data, and refitted models. These predictors cause extreme extrapolations of high density offshore in April and May in unsurveyed waters. Model released as part of a scheduled update to the U.S. Navy Marine Species Density Database (NMSDD).

*For questions or to offer feedback please contact Jason Roberts (jason.roberts@duke.edu) and Tina Yack (tina.yack@duke.edu)

(continued)

Version	Date	Description
7	2022-06-20	This model is a major update over the prior version, with substantial additional data, improved statistical methods, and an increased spatial resolution. It was released as part of the final delivery of the U.S. Navy Marine Species Density Database (NMSDD) for the Atlantic Fleet Testing and Training (AFTT) Phase IV Environmental Impact Statement. Several new collaborators joined and contributed survey data: New York State Department of Environmental Conservation, TetraTech, HDR, and Marine Conservation Research. We incorporated additional surveys from all continuing and new collaborators through the end of 2020. (Because some environmental covariates were only available through 2019, certain models only extend through 2019.) We increased the spatial resolution to 5 km and, at NOAA's request, we extended the model further inshore from New York through Maine. We reformulated and refitted all detection functions and spatial models. We updated all environmental covariates to newer products, when available, and added several covariates to the set of candidates. For models that incorporated dynamic covariates, we estimated model uncertainty using a new method that accounts for both model parameter error and temporal variability.
7.1	2023-05-27	Completed the supplementary report documenting the details of this model. The model itself was not changed.

1 Survey Data

We built this model from data collected between 2010-2019 (Table 1, Figure 1). In order to be consistent with other beaked whale models and due to increased efforts and abilities to identify beaked whales in more recent years, we elected to exclude data prior to 2010. We also excluded data after 2019 in order to utilize zooplankton and micronekton biomass estimates from SEAPODYM (Lehodey et al. 2008), which preliminary modeling indicated were effective spatial covariates but were only available through 2019. Further, we excluded surveys that did not include beaked whales within their list of target species. We restricted the model to survey transects with sea states of Beaufort 5 or less (for a few surveys we used Beaufort 4 or less) for both aerial and shipboard surveys. We also excluded transects with poor weather or visibility for surveys that reported those conditions.

Table 1: Survey effort and observations considered for this model. Effort is tallied as the cumulative length of on-effort transects. Observations are the number of groups and individuals encountered while on effort. Off effort observations and those lacking an estimate of group size or distance to the group were excluded.

Institution	Program	Period	Effort	Observations		
			1000s km	Groups	Individuals	Mean Group Size
Aerial Surveys						
HDR	Navy Norfolk Canyon	2018-2019	11	4	7	1.8
NEAq	CNM	2017-2019	2	0	0	
NEAq	MMS-WEA	2017-2019	31	0	0	
NEAq	NLPSC	2011-2015	43	0	0	
NEFSC	AMAPPS	2010-2019	89	10	19	1.9
NEFSC	NARWSS	2010-2019	200	3	4	1.3
NYS-DEC/TT	NYBWM	2017-2019	58	2	7	3.5
SEFSC	AMAPPS	2010-2019	111	2	2	1.0
UNCW	Navy Cape Hatteras	2011-2017	34	0	0	
UNCW	Navy Jacksonville	2010-2017	76	0	0	
UNCW	Navy Norfolk Canyon	2015-2017	14	0	0	
UNCW	Navy Onslow Bay	2010-2011	14	0	0	
VAMSC	MD DNR WEA	2013-2015	16	0	0	
VAMSC	Navy VACAPES	2016-2017	19	0	0	
VAMSC	VA CZM WEA	2012-2015	21	0	0	
		Total	740	21	39	1.9
Shipboard Surveys						
NEFSC	AMAPPS	2011-2016	14	66	148	2.2
SEFSC	AMAPPS	2011-2016	14	31	63	2.0
		Total	29	97	211	2.2
		Grand Total	769	118	250	2.1

Table 2: Institutions that contributed surveys used in this model.

Institution	Full Name
HDR	HDR, Inc.
NEAq	New England Aquarium
NEFSC	NOAA Northeast Fisheries Science Center
NYS-DEC/TT	New York State Department of Environmental Conservation and Tetra Tech, Inc.
SEFSC	NOAA Southeast Fisheries Science Center
UNCW	University of North Carolina Wilmington
VAMSC	Virginia Aquarium & Marine Science Center

Table 3: Descriptions and references for survey programs used in this model.

Program	Description	References
AMAPPS	Atlantic Marine Assessment Program for Protected Species	Palka et al. (2017), Palka et al. (2021)
CNM	Northeast Canyons Marine National Monument Aerial Surveys	Redfern et al. (2021)
MD DNR WEA	Aerial Surveys of the Maryland Wind Energy Area	Barco et al. (2015)
MMS-WEA	Marine Mammal Surveys of the MA and RI Wind Energy Areas	Quintana-Rizzo et al. (2021), O'Brien et al. (2022)
NARWSS	North Atlantic Right Whale Sighting Surveys	Cole et al. (2007)
Navy Cape Hatteras	Aerial Surveys of the Navy's Cape Hatteras Study Area	McLellan et al. (2018)
Navy Jacksonville	Aerial Surveys of the Navy's Jacksonville Study Area	Foley et al. (2019)
Navy Norfolk Canyon	Aerial Surveys of the Navy's Norfolk Canyon Study Area	Cotter (2019), McAlarney et al. (2018)
Navy Onslow Bay	Aerial Surveys of the Navy's Onslow Bay Study Area	Read et al. (2014)
Navy VACAPES	Aerial Survey Baseline Monitoring in the Continental Shelf Region of the VACAPES OPAREA	Malette et al. (2017)
NLPSC	Northeast Large Pelagic Survey Collaborative Aerial Surveys	Leiter et al. (2017), Stone et al. (2017)
NYBWM	New York Bight Whale Monitoring Surveys	Zoidis et al. (2021)
VA CZM WEA	Virginia CZM Wind Energy Area Surveys	Malette et al. (2014), Malette et al. (2015)

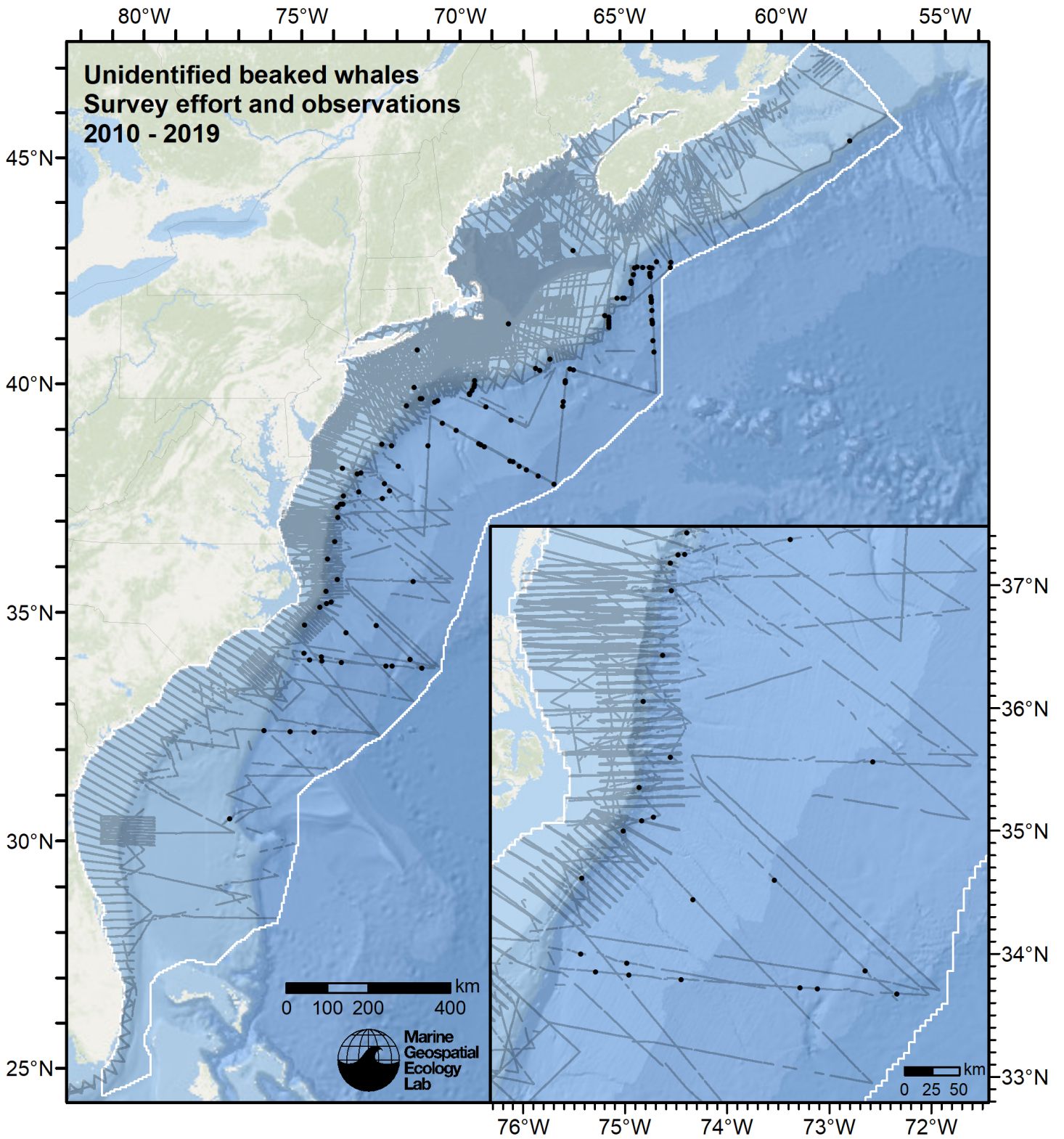


Figure 1: Survey effort and unidentified beaked whales observations available for density modeling, after detection functions were applied, and excluded segments and truncated observations were removed.

2 Detection Functions

2.1 With a Taxonomic Covariate

We fitted the detection functions in this section to pools of species with similar detectability characteristics and used the taxonomic identification as a covariate (ScientificName) to account for differences between them. We consulted the literature and observer teams to determine appropriate poolings. We usually employed this approach to boost the counts of observations in the detection functions, which increased the chance that other covariates such as Beaufort sea state could be used to account for differences in observing conditions. When defining the taxonomic covariate, we sometimes had too few observations of species to allocate each of them their own level of the covariate and had to group them together, again consulting the literature and observers for advice on species similarity. Also, when species were observed frequently enough to be allocated their own levels but statistical tests indicated no significant difference between the levels, we usually grouped them together into a single level.

2.1.1 Beaked and Kogia Whales

2.1.1.1 Aerial Surveys

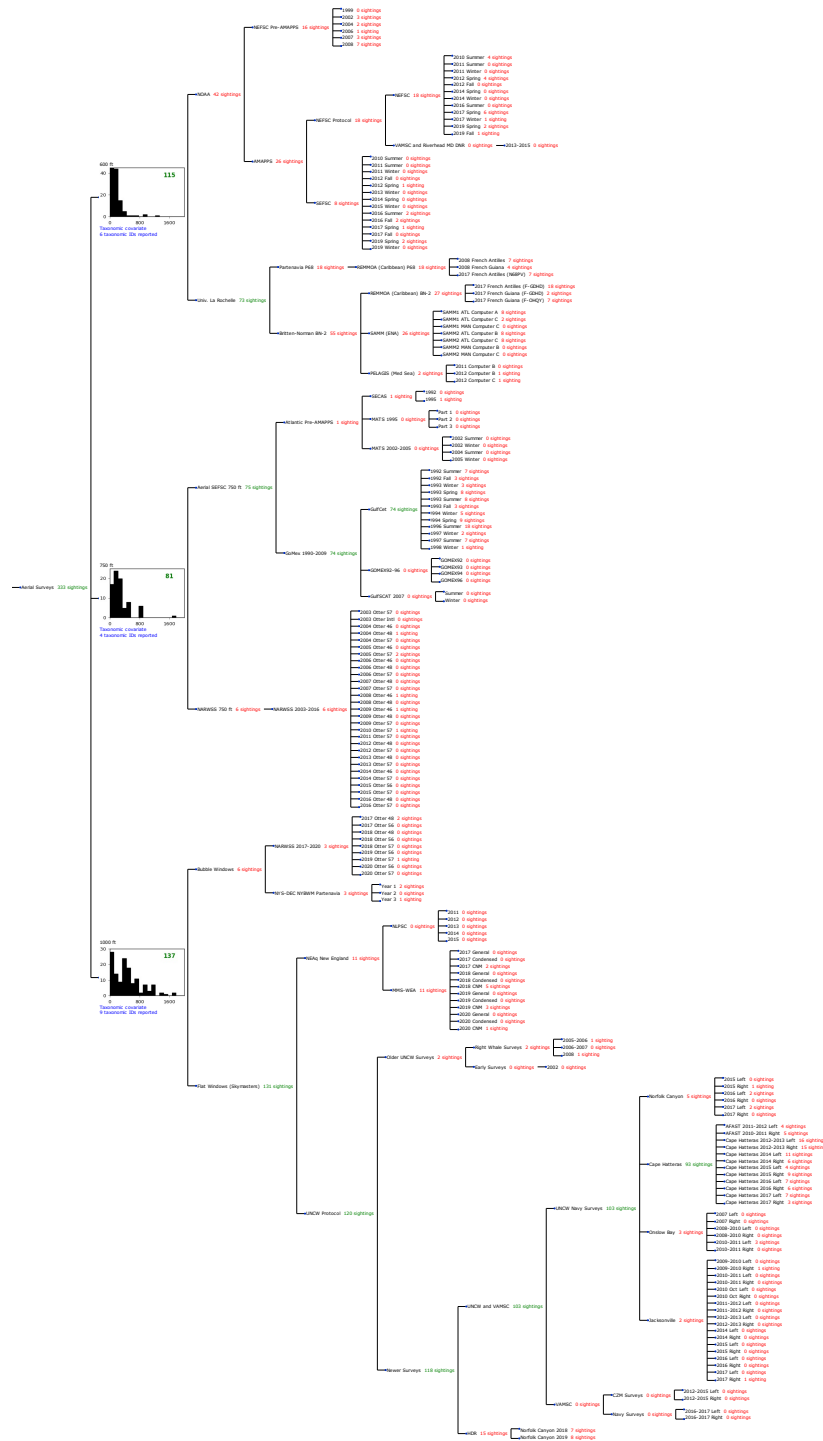


Figure 2: Detection hierarchy for aerial surveys, showing how they were pooled during detectability modeling, for detection functions that pooled multiple taxa and used a taxonomic covariate to account for differences between them. Each histogram represents a detection function and summarizes the perpendicular distances of observations that were pooled to fit it, prior to truncation. Observation counts, also prior to truncation, are shown in green when they met the recommendation of Buckland et al. (2001) that detection functions utilize at least 60 sightings, and red otherwise. For rare taxa, it was not always possible to meet this recommendation, yielding higher statistical uncertainty. During the spatial modeling stage of the analysis, effective strip widths were computed for each survey using the closest detection function above it in the hierarchy (i.e. moving from right to left in the figure). Surveys that do not have a detection function above them in this figure were either addressed by a detection function presented in a different section of this report, or were omitted from the analysis.

2.1.1.1.1 600 ft

After right-truncating observations greater than 400 m, we fitted the detection function to the 109 observations that remained (Table 4). The selected detection function (Figure 3) used a hazard rate key function with OriginalScientificName (Figure 4) as a covariate.

Table 4: Observations used to fit the 600 ft detection function.

ScientificName	n
Hyperoodon ampullatus	3
Kogia	23
Mesoplodon	14
Mesoplodon bidens	1
Ziphiidae	33
Ziphius cavirostris	35
Total	109

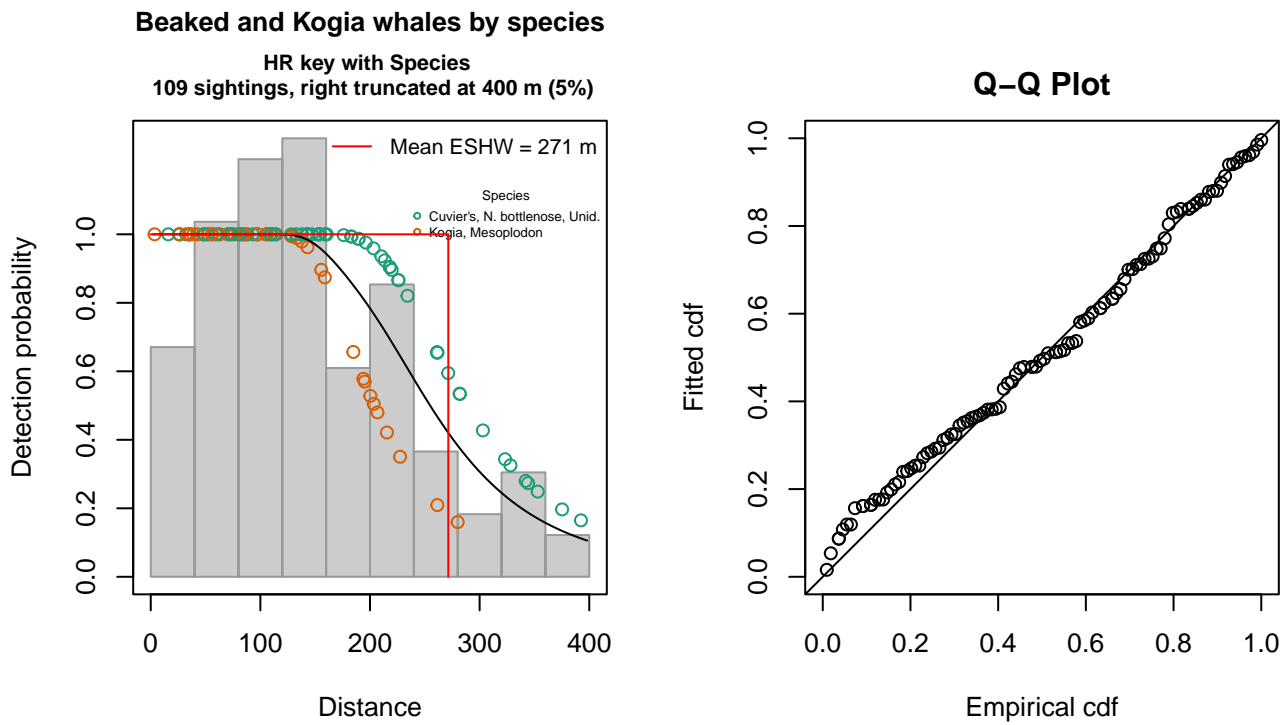


Figure 3: 600 ft detection function and Q-Q plot showing its goodness of fit.

Statistical output for this detection function:

Summary for ds object

Number of observations : 109
 Distance range : 0 - 400
 AIC : 1272.901

Detection function:

Hazard-rate key function

Detection function parameters

Scale coefficient(s):

	estimate	se
(Intercept)	5.5800164	0.1212472

OriginalScientificNameKogia, Mesoplodon -0.3454612 0.1492241

Shape coefficient(s):

	estimate	se
(Intercept)	1.474338	0.3977595

	Estimate	SE	CV
Average p	0.6645919	0.04555694	0.06854874
N in covered region	164.0104361	14.58154672	0.08890621

Distance sampling Cramer-von Mises test (unweighted)

Test statistic = 0.116256 p = 0.510907

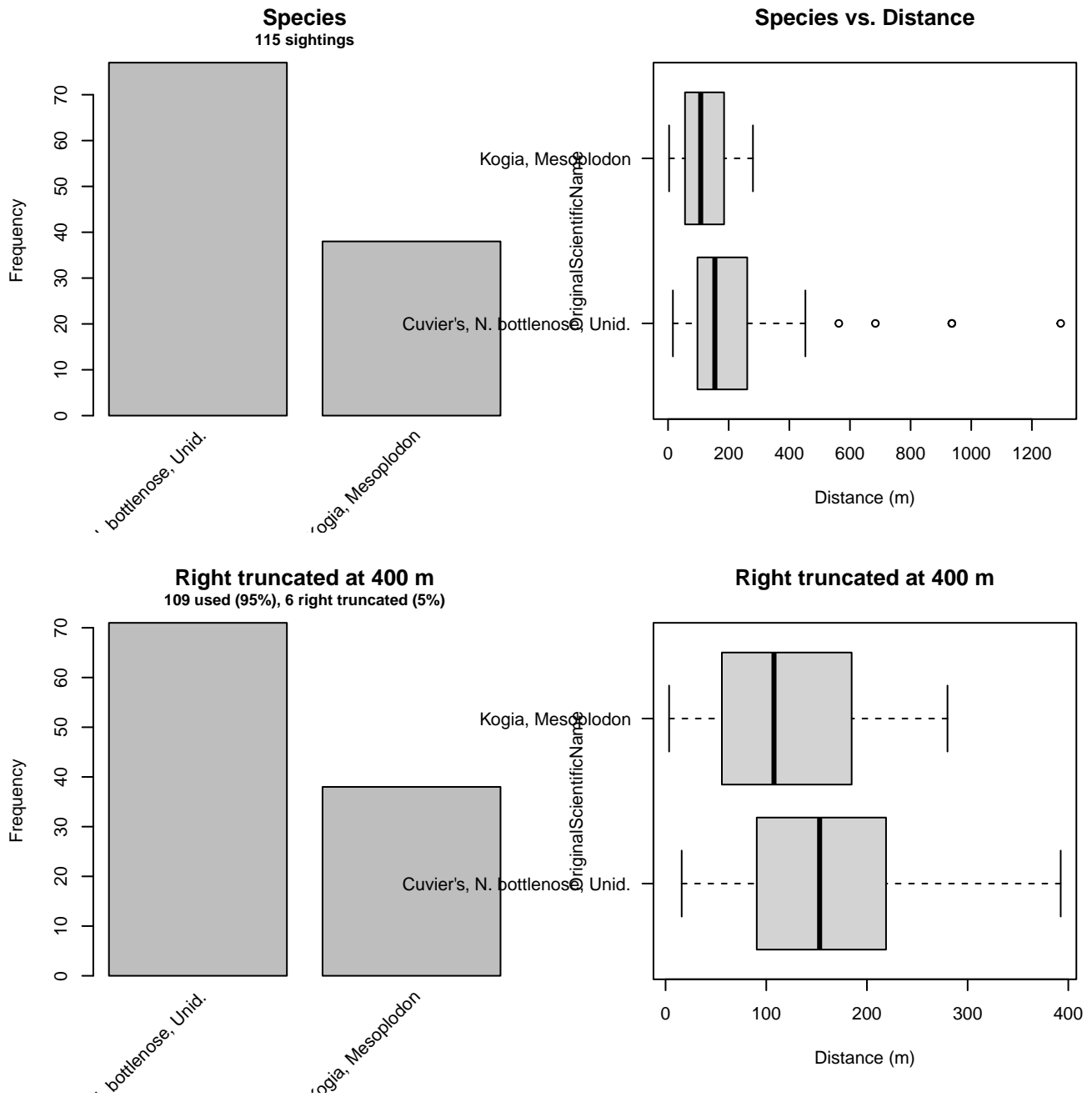


Figure 4: Distribution of the OriginalScientificName covariate before (top row) and after (bottom row) observations were truncated to fit the 600 ft detection function.

2.1.1.1.2 750 ft

After right-truncating observations greater than 1297 m, we fitted the detection function to the 80 observations that remained (Table 5). The selected detection function (Figure 5) used a hazard rate key function with Beaufort (Figure 6) and OriginalScientificName (Figure 7) as covariates.

Table 5: Observations used to fit the 750 ft detection function.

ScientificName	n
Kogia	55
Mesoplodon	9
Ziphiidae	12
Ziphius cavirostris	4
Total	80

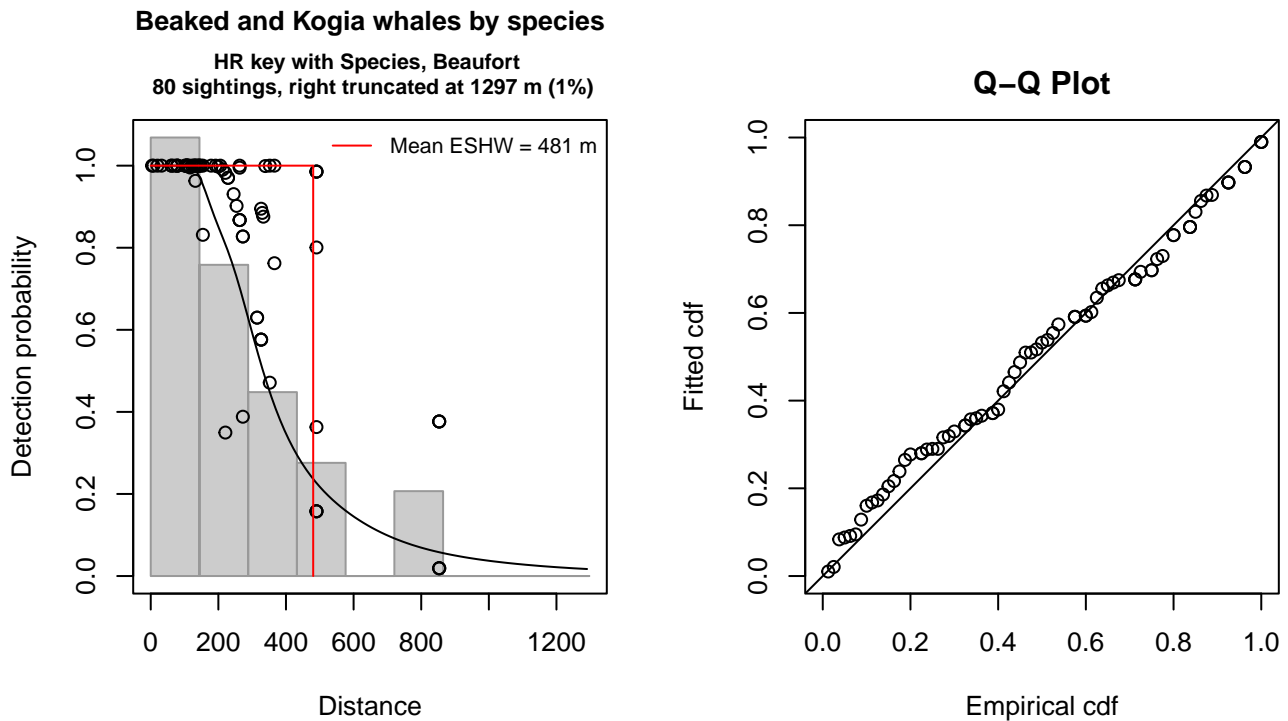


Figure 5: 750 ft detection function and Q-Q plot showing its goodness of fit.

Statistical output for this detection function:

Summary for ds object

Number of observations : 80
 Distance range : 0 - 1297
 AIC : 1037.791

Detection function:

Hazard-rate key function

Detection function parameters

Scale coefficient(s):

	estimate	se
(Intercept)	7.1253756	0.3142159
OriginalScientificNameKogia	-0.8097794	0.2203485
Beaufort	-0.5658239	0.1695498

Shape coefficient(s):

	estimate	se
(Intercept)	1.375855	0.1977036

	Estimate	SE	CV
Average p	0.3064062	0.03275229	0.1068917
N in covered region	261.0913218	37.74245080	0.1445565

Distance sampling Cramer-von Mises test (unweighted)
Test statistic = 0.106921 p = 0.551997

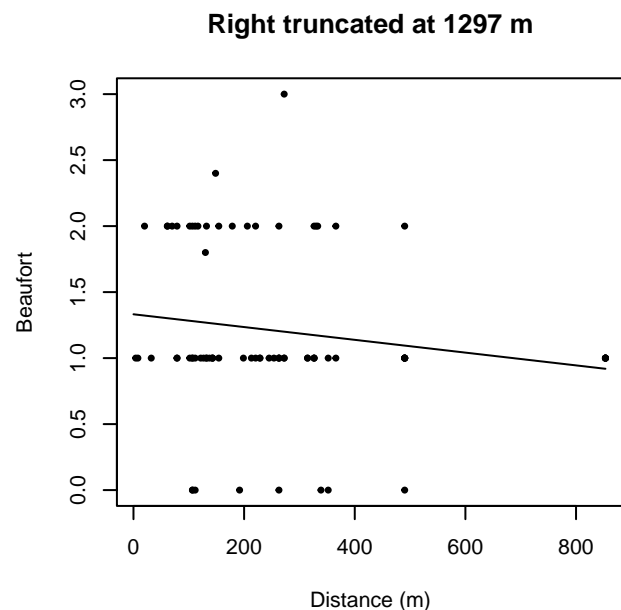
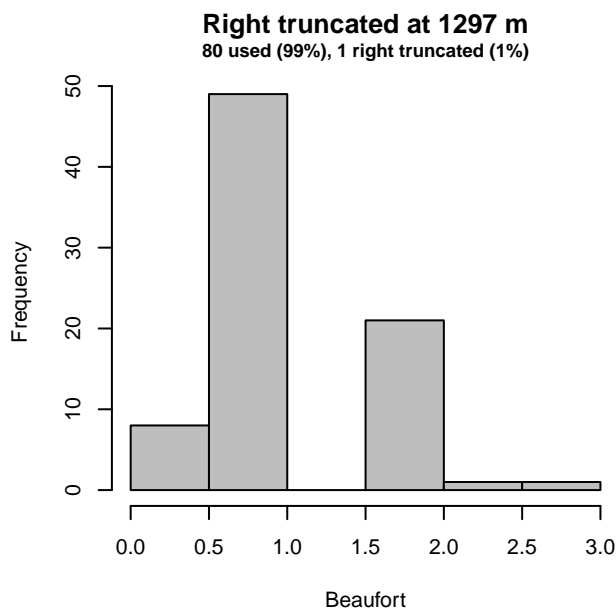
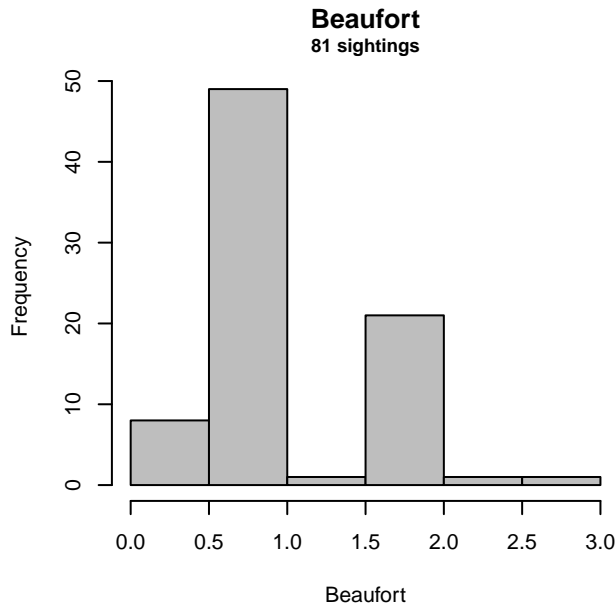


Figure 6: Distribution of the Beaufort covariate before (top row) and after (bottom row) observations were truncated to fit the 750 ft detection function.

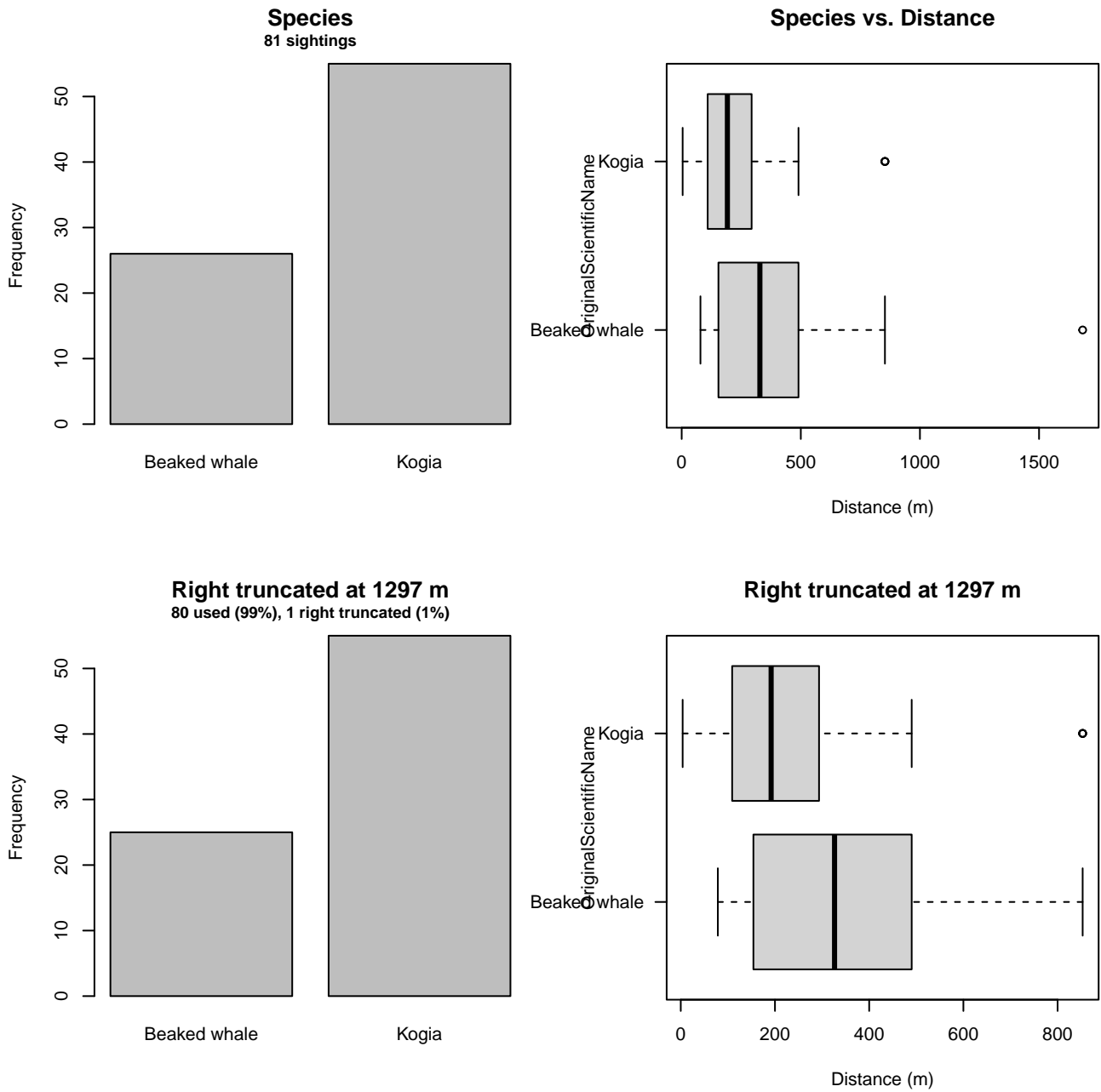


Figure 7: Distribution of the OriginalScientificName covariate before (top row) and after (bottom row) observations were truncated to fit the 750 ft detection function.

2.1.1.1.3 1000 ft

After right-truncating observations greater than 1250 m, we fitted the detection function to the 131 observations that remained (Table 6). The selected detection function (Figure 8) used a half normal key function with OriginalScientificName (Figure 9) as a covariate.

Table 6: Observations used to fit the 1000 ft detection function.

ScientificName	n
Hyperoodon ampullatus	1
Kogia	14
Kogia sima	1
Mesoplodon	26
Mesoplodon bidens	6
Mesoplodon europaeus	7
Mesoplodon mirus	3
Ziphiidae	11
Ziphius cavirostris	62
Total	131

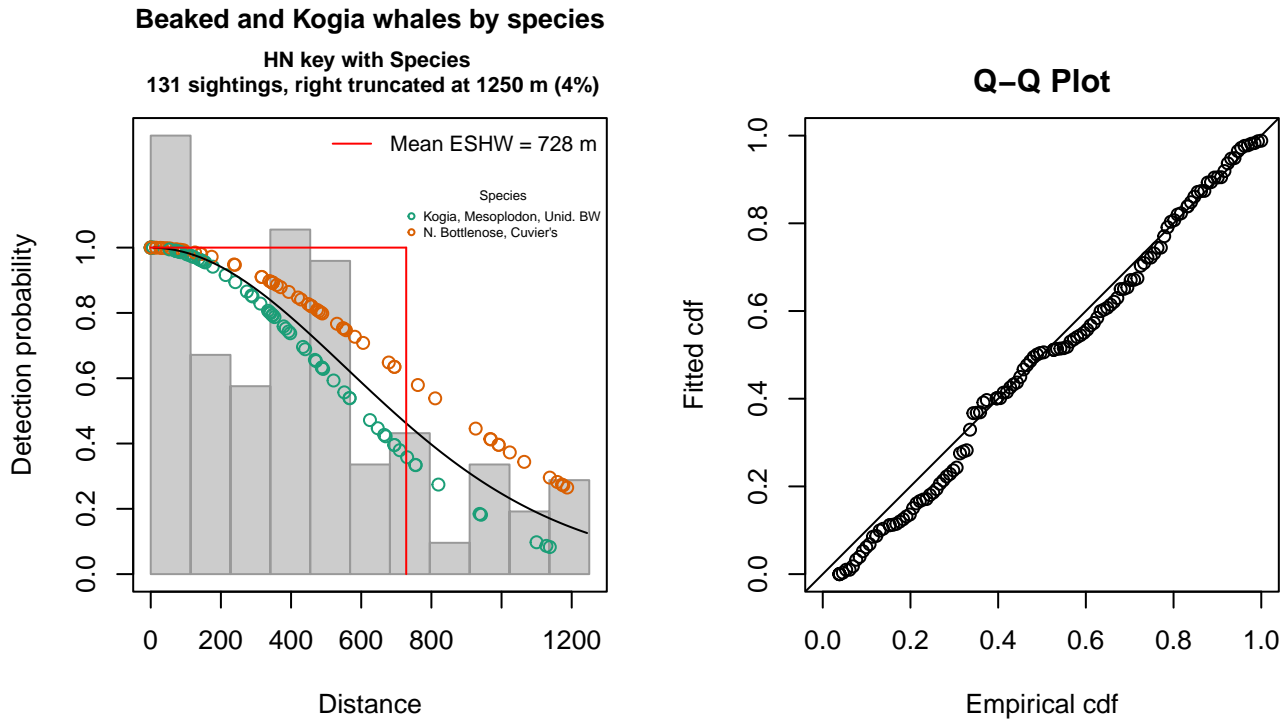


Figure 8: 1000 ft detection function and Q-Q plot showing its goodness of fit.

Statistical output for this detection function:

Summary for ds object

Number of observations : 131
 Distance range : 0 - 1250
 AIC : 1830.819

Detection function:

Half-normal key function

Detection function parameters

Scale coefficient(s):

	estimate	se
(Intercept)	6.2340705	0.1031336
OriginalScientificNameN. Bottlenose, Cuvier's	0.3570255	0.1899459

Estimate	SE	CV
----------	----	----

Average p 0.5712474 0.04000868 0.07003740
 N in covered region 229.3227075 20.84792919 0.09091088

Distance sampling Cramer-von Mises test (unweighted)
 Test statistic = 0.133457 p = 0.444164

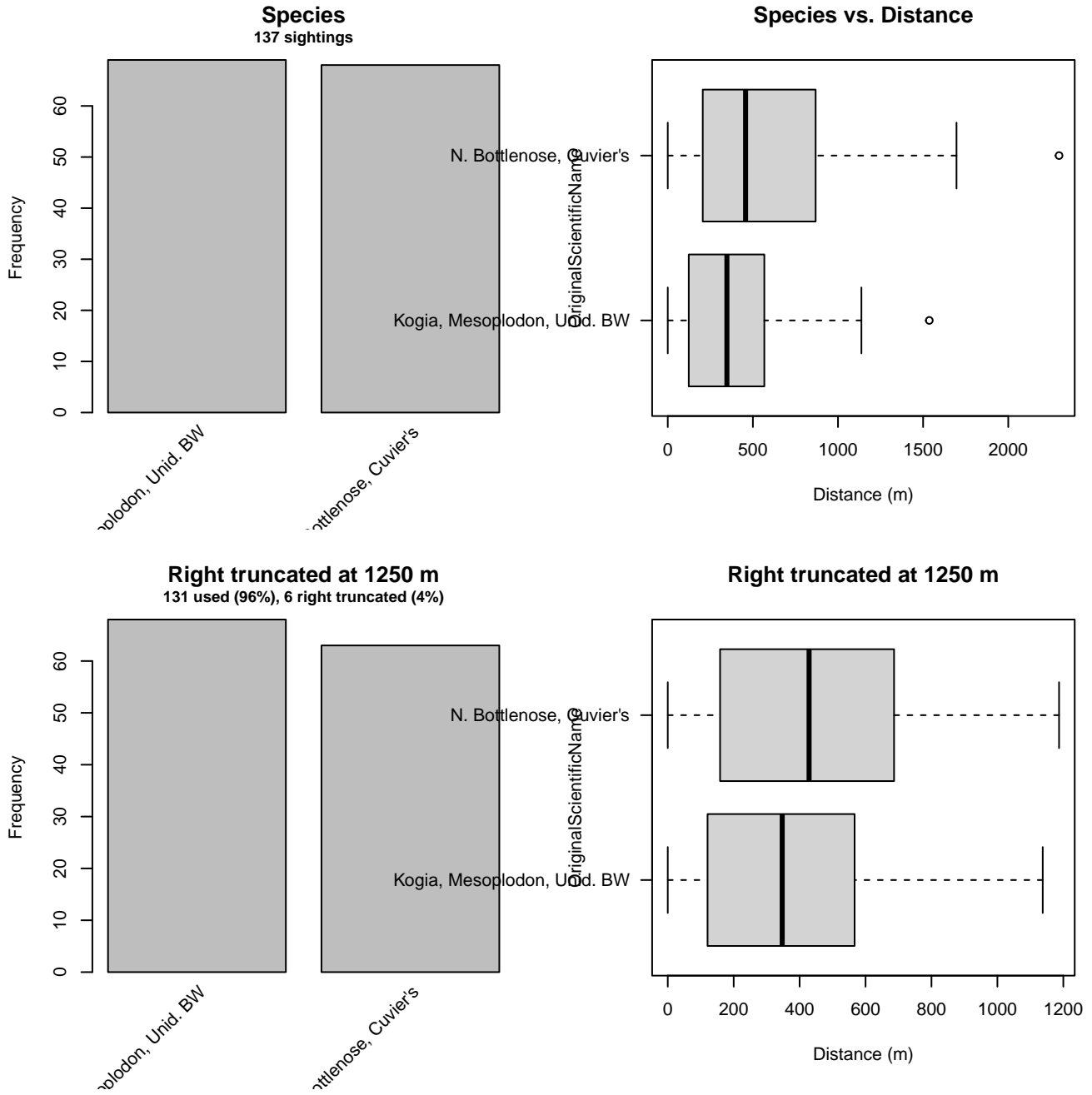


Figure 9: Distribution of the OriginalScientificName covariate before (top row) and after (bottom row) observations were truncated to fit the 1000 ft detection function.

2.1.1.2 Shipboard Surveys

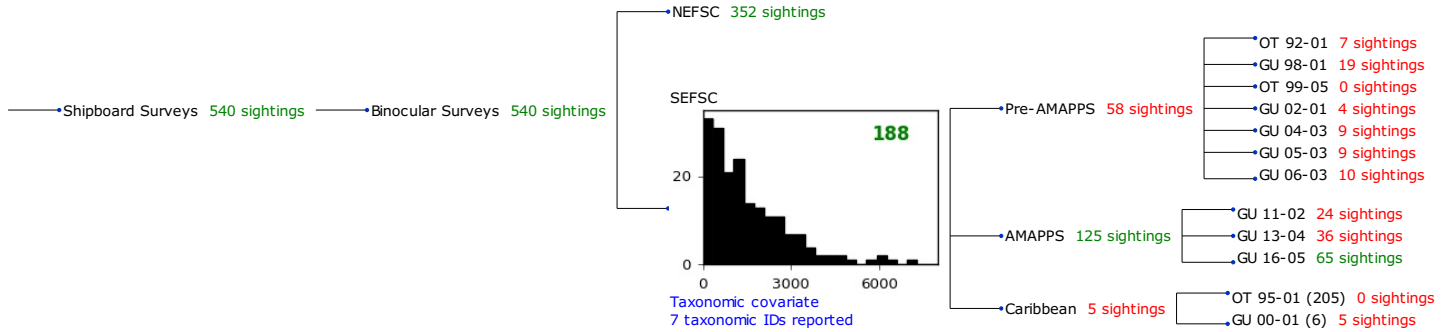


Figure 10: Detection hierarchy for shipboard surveys, showing how they were pooled during detectability modeling, for detection functions that pooled multiple taxa and used a taxonomic covariate to account for differences between them. Each histogram represents a detection function and summarizes the perpendicular distances of observations that were pooled to fit it, prior to truncation. Observation counts, also prior to truncation, are shown in green when they met the recommendation of Buckland et al. (2001) that detection functions utilize at least 60 sightings, and red otherwise. For rare taxa, it was not always possible to meet this recommendation, yielding higher statistical uncertainty. During the spatial modeling stage of the analysis, effective strip widths were computed for each survey using the closest detection function above it in the hierarchy (i.e. moving from right to left in the figure). Surveys that do not have a detection function above them in this figure were either addressed by a detection function presented in a different section of this report, or were omitted from the analysis.

2.1.1.2.1 SEFSC

After right-truncating observations greater than 5000 m, we fitted the detection function to the 182 observations that remained (Table 7). The selected detection function (Figure 11) used a half normal key function with Beaufort (Figure 12) and OriginalScientificName (Figure 13) as covariates.

Table 7: Observations used to fit the SEFSC detection function.

ScientificName	n
Kogia	60
Kogia sima	9
Mesoplodon	37
Mesoplodon densirostris	3
Mesoplodon europaeus	1
Ziphiidae	52
Ziphius cavirostris	20
Total	182

Beaked and Kogia whales by species

HN key with Species, Beaufort
182 sightings, right truncated at 5000 m (3%)

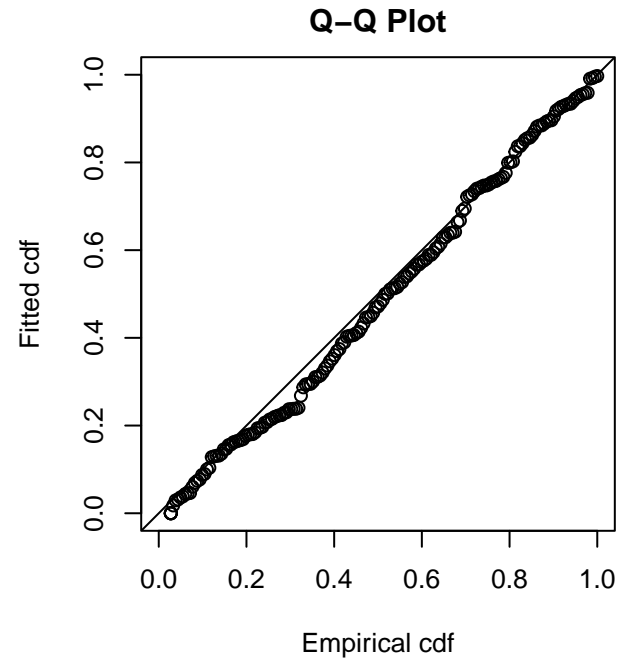
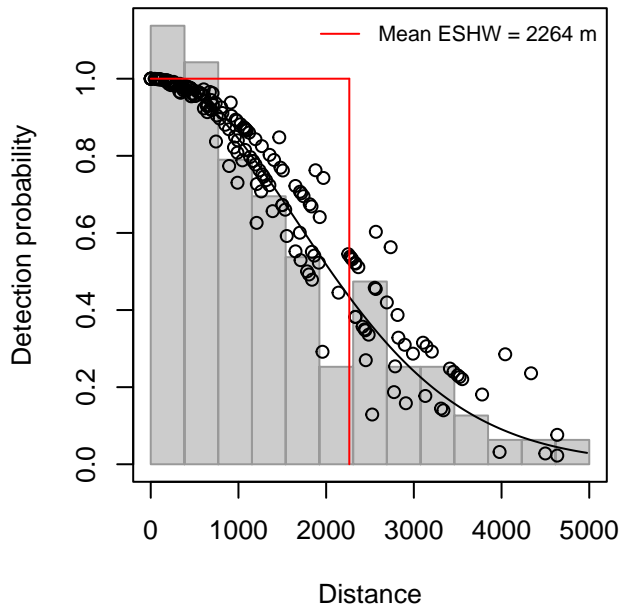


Figure 11: SEFSC detection function and Q-Q plot showing its goodness of fit.

Statistical output for this detection function:

Summary for ds object

Number of observations : 182
Distance range : 0 - 5000
AIC : 2985.886

Detection function:

Half-normal key function

Detection function parameters

Scale coefficient(s):

	estimate
(Intercept)	7.4282169
OriginalScientificNameMesoplodon spp. and Unid. beaked whale	0.1940795
OriginalScientificNameZiphius or N. bottlenose	0.4163007
Beaufort3-4	-0.2991956
	se
(Intercept)	0.08116764
OriginalScientificNameMesoplodon spp. and Unid. beaked whale	0.12604909
OriginalScientificNameZiphius or N. bottlenose	0.24124124
Beaufort3-4	0.13661134

	Estimate	SE	CV
Average p	0.4423162	0.02407533	0.05443013
N in covered region	411.4703239	32.09594942	0.07800307

Distance sampling Cramer-von Mises test (unweighted)

Test statistic = 0.128965 p = 0.460545

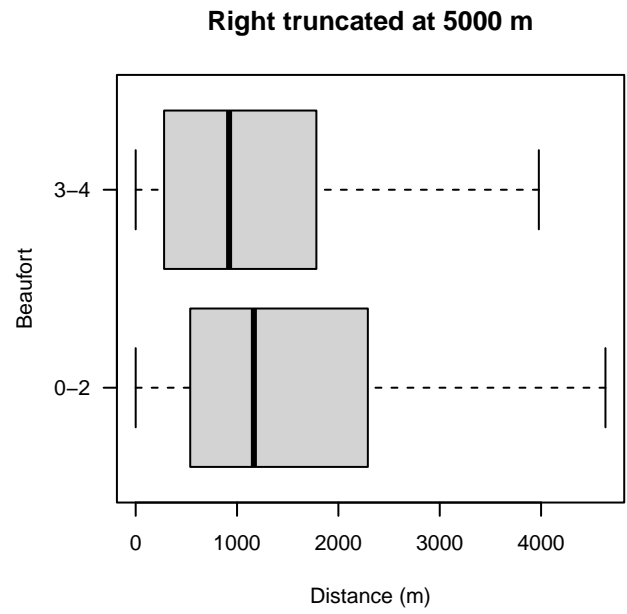
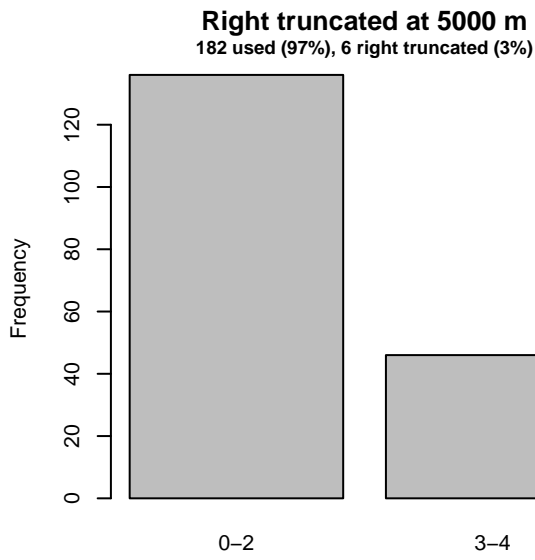
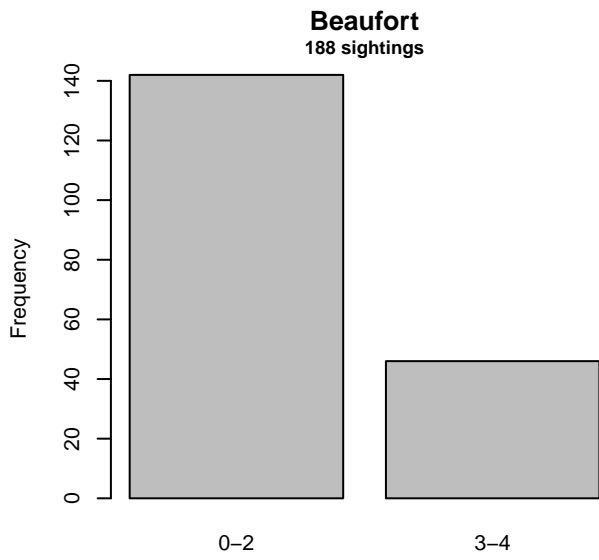


Figure 12: Distribution of the Beaufort covariate before (top row) and after (bottom row) observations were truncated to fit the SEFSC detection function.

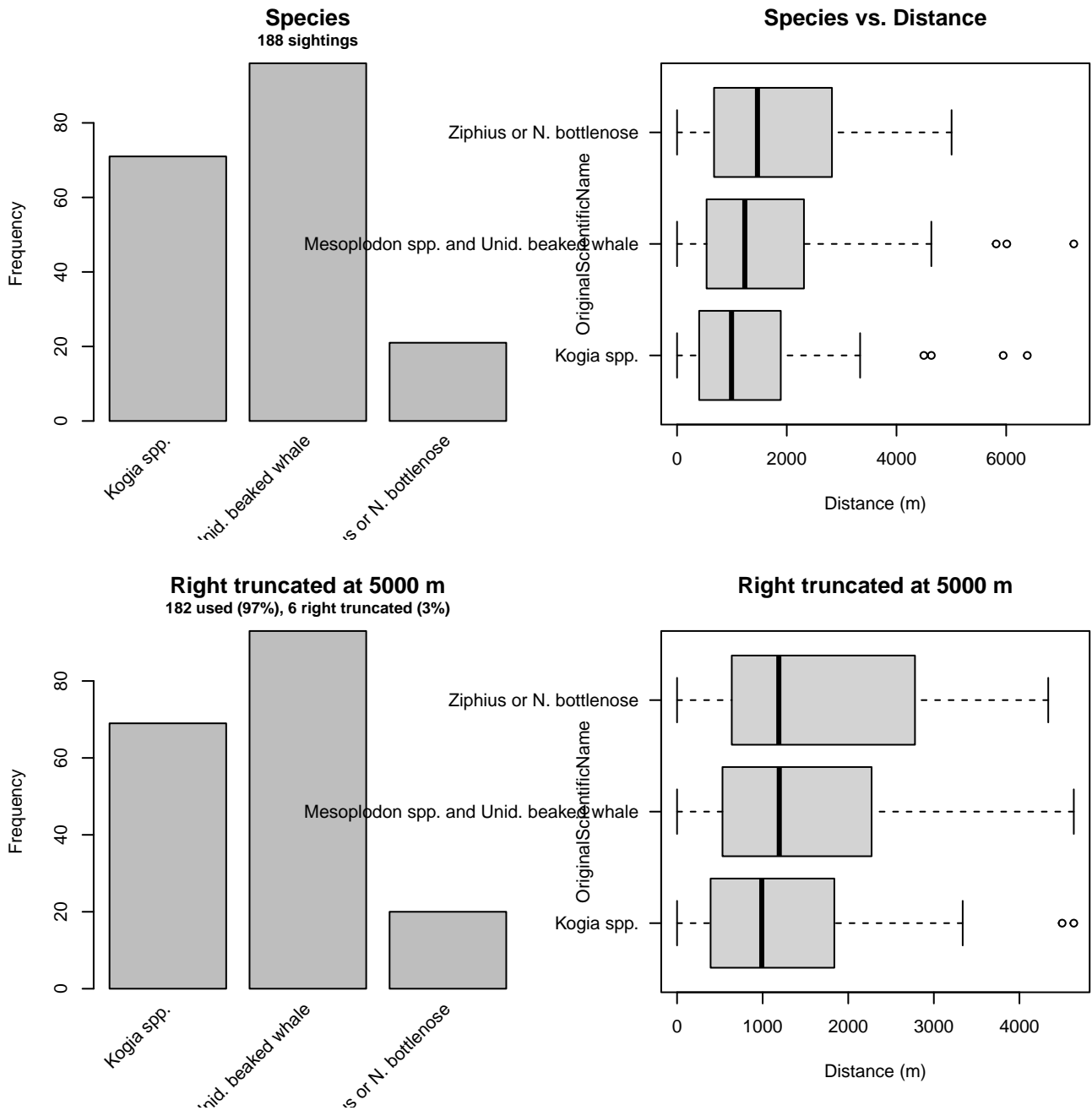


Figure 13: Distribution of the OriginalScientificName covariate before (top row) and after (bottom row) observations were truncated to fit the SEFSC detection function.

2.1.2 Beaked Whales

2.1.2.1 Shipboard Surveys

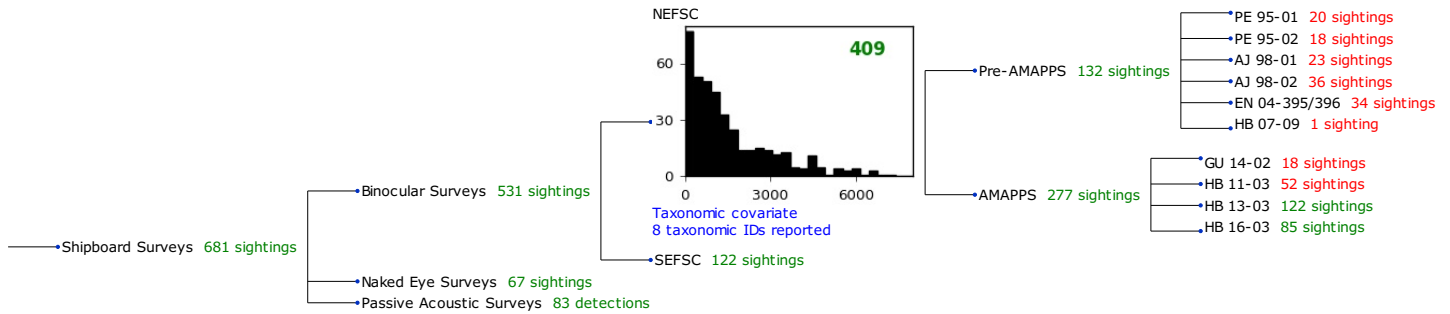


Figure 14: Detection hierarchy for shipboard surveys, showing how they were pooled during detectability modeling, for detection functions that pooled multiple taxa and used a taxonomic covariate to account for differences between them. Each histogram represents a detection function and summarizes the perpendicular distances of observations that were pooled to fit it, prior to truncation. Observation counts, also prior to truncation, are shown in green when they met the recommendation of Buckland et al. (2001) that detection functions utilize at least 60 sightings, and red otherwise. For rare taxa, it was not always possible to meet this recommendation, yielding higher statistical uncertainty. During the spatial modeling stage of the analysis, effective strip widths were computed for each survey using the closest detection function above it in the hierarchy (i.e. moving from right to left in the figure). Surveys that do not have a detection function above them in this figure were either addressed by a detection function presented in a different section of this report, or were omitted from the analysis.

2.1.2.1.1 NEFSC

After right-truncating observations greater than 6000 m, we fitted the detection function to the 402 observations that remained (Table 8). The selected detection function (Figure 15) used a hazard rate key function with Beaufort (Figure 16), OriginalScientificName (Figure 17) and VesselName (Figure 18) as covariates.

Table 8: Observations used to fit the NEFSC detection function.

ScientificName	n
Hyperoodon ampullatus	4
Mesoplodon	69
Mesoplodon bidens	40
Mesoplodon densirostris	4
Mesoplodon europaeus	9
Mesoplodon mirus	7
Ziphiidae	147
Ziphius cavirostris	122
Total	402

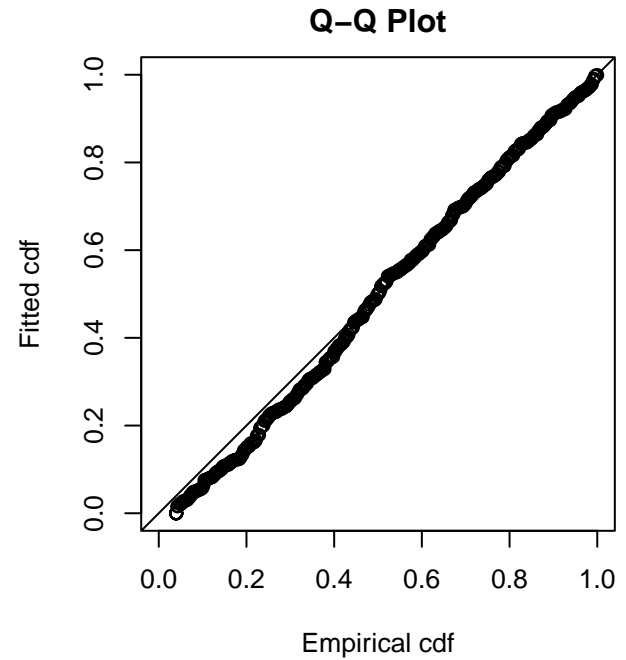
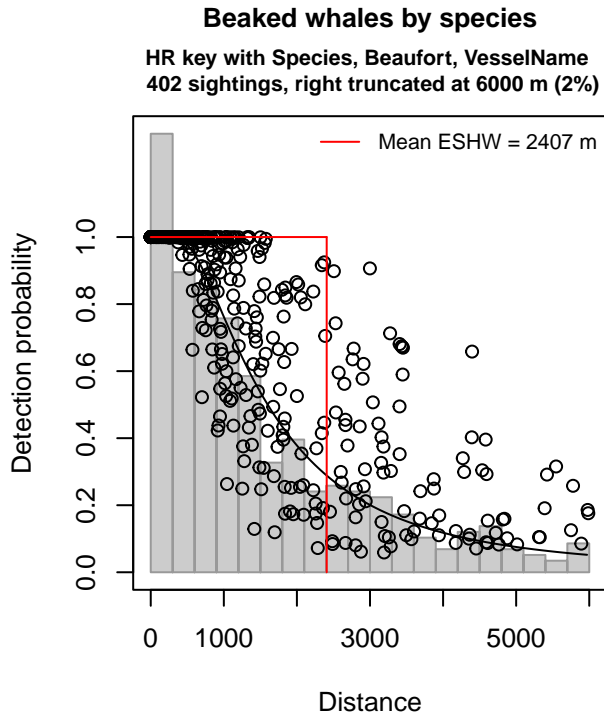


Figure 15: NEFSC detection function and Q-Q plot showing its goodness of fit.

Statistical output for this detection function:

Summary for ds object

Number of observations : 402
 Distance range : 0 - 6000
 AIC : 6644.8

Detection function:

Hazard-rate key function

Detection function parameters

Scale coefficient(s):

	estimate	se
(Intercept)	7.2946616	0.23066680
OriginalScientificNameN. Bottlenose or Unid. beaked whale	0.4273741	0.15634310
OriginalScientificNameZiphius cavirostris	0.2066261	0.14919980
Beaufort	-0.3259831	0.06466977
VesselNameBigelow, Endeavor, Gunter	0.7959452	0.15617439

Shape coefficient(s):

	estimate	se
(Intercept)	0.8157154	0.1116931

	Estimate	SE	CV
Average p	0.3459974	0.02233711	0.06455861
N in covered region	1161.8584040	89.48657432	0.07702021

Distance sampling Cramer-von Mises test (unweighted)

Test statistic = 0.276181 p = 0.158010

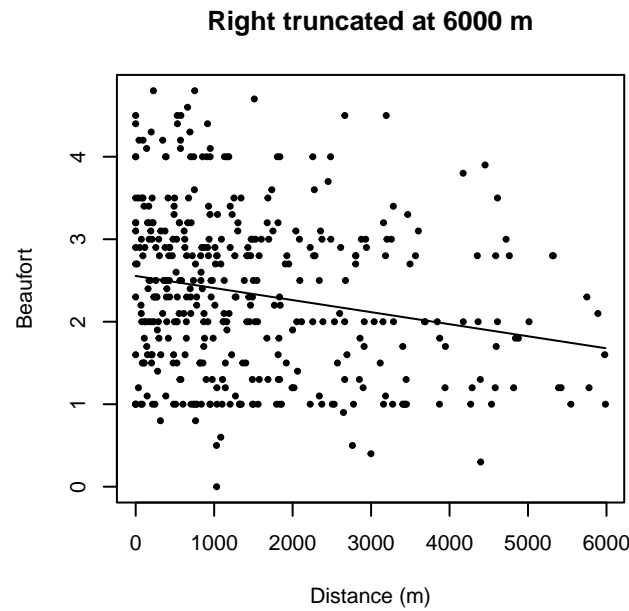
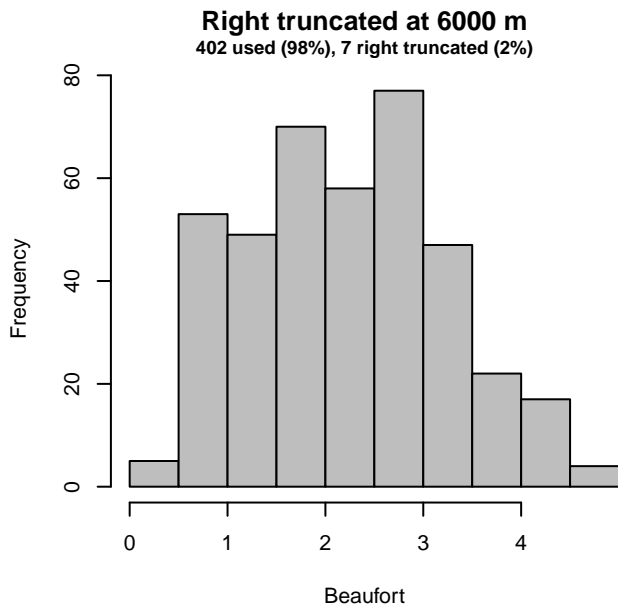
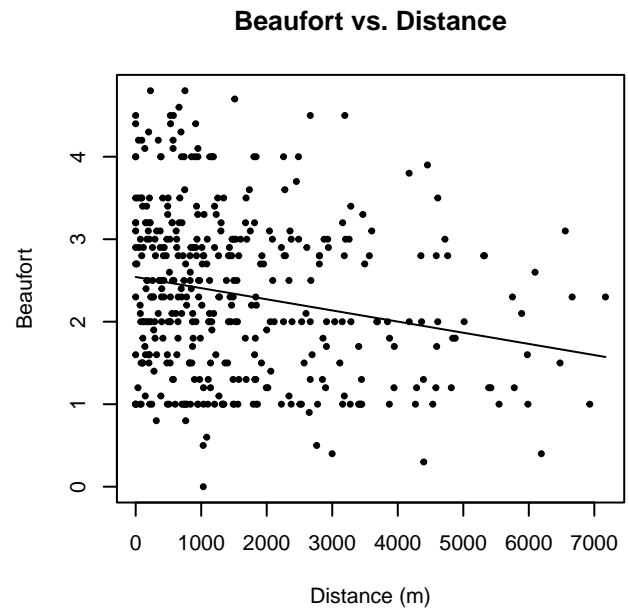
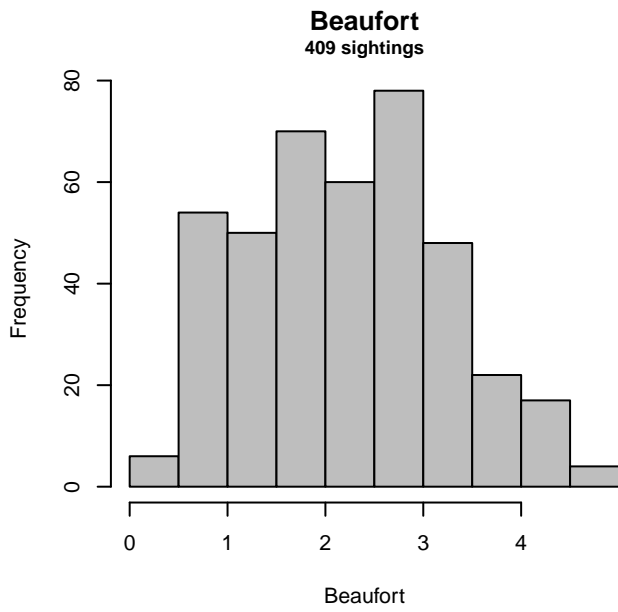


Figure 16: Distribution of the Beaufort covariate before (top row) and after (bottom row) observations were truncated to fit the NEFSC detection function.

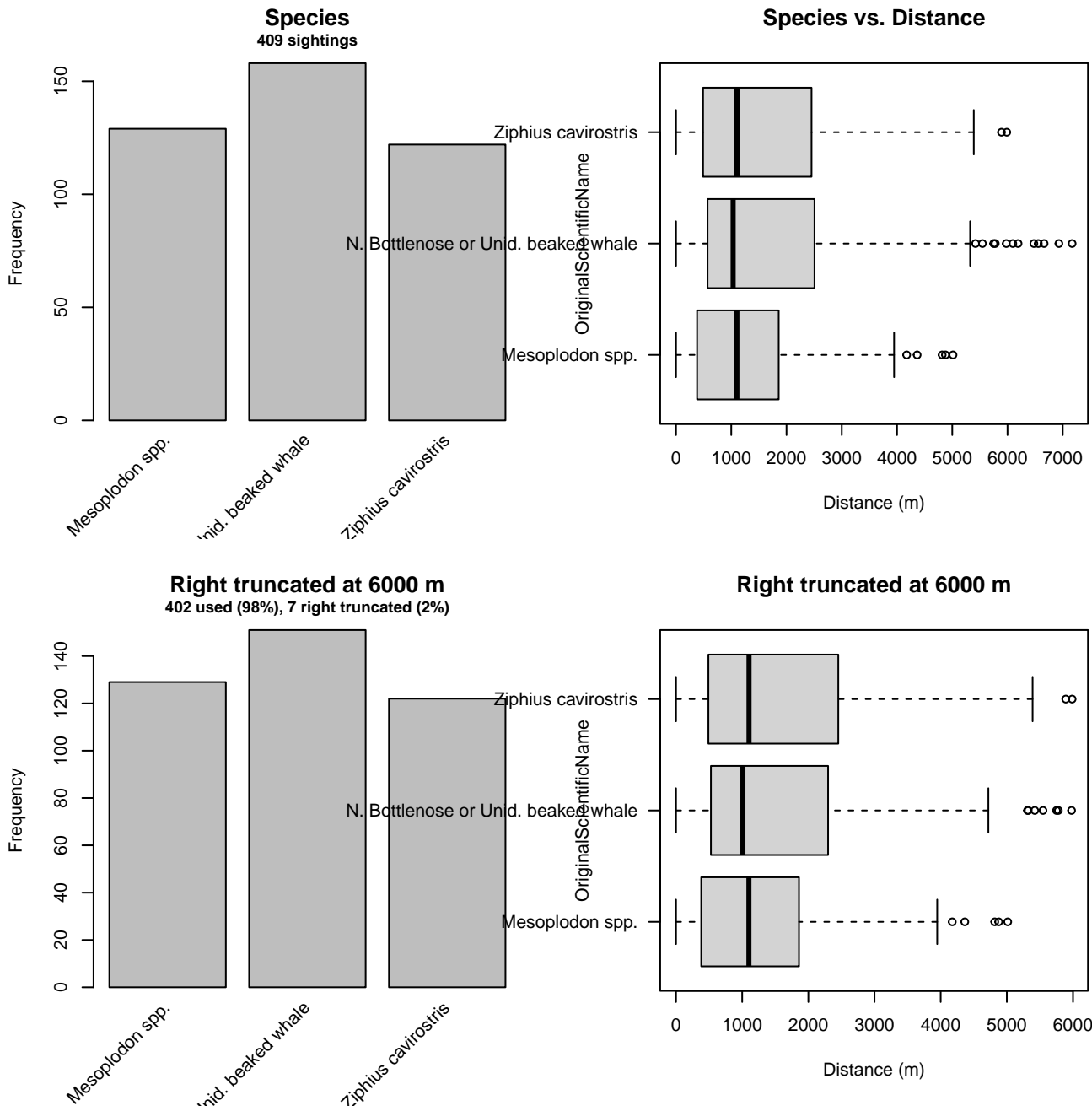


Figure 17: Distribution of the OriginalScientificName covariate before (top row) and after (bottom row) observations were truncated to fit the NEFSC detection function.

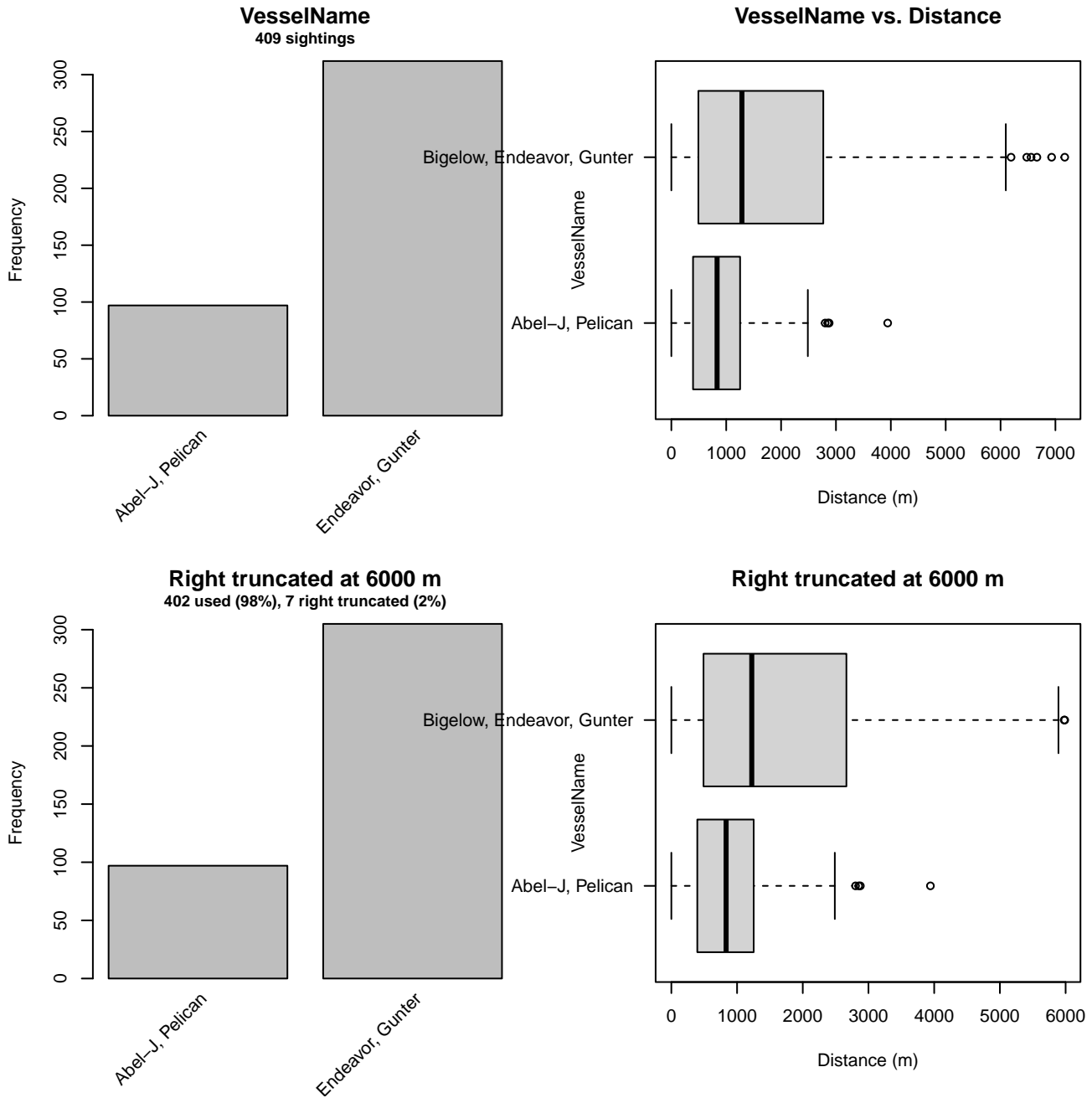


Figure 18: Distribution of the VesselName covariate before (top row) and after (bottom row) observations were truncated to fit the NEFSC detection function.

3 Bias Corrections

Density surface modeling methodology uses *distance sampling* (Buckland et al. 2001) to model the probability that an observer on a line transect survey will detect an animal given the perpendicular distance to it from the transect line. Distance sampling assumes that detection probability is 1 when perpendicular distance is 0. When this assumption is not met, detection probability is biased high, leading to an underestimation of density and abundance. This is known as the $g_0 < 1$ problem, where g_0 refers to the detection probability at distance 0. Modelers often try to address this problem by estimating g_0 empirically and dividing it into estimated density or abundance, thereby correcting those estimates to account for the animals that were presumed missed.

Two important sources of bias for visual surveys are known as *availability bias*, in which an animal was present on the transect line but impossible to detect, e.g. because it was under water, and *perception bias*, in which an animal was present and available but not noticed, e.g. because of its small size or cryptic coloration or behavior (Marsh and Sinclair 1989). Modelers often

estimate the influence of these two sources of bias on detection probability independently, yielding two estimates of g_0 , hereafter referred to as g_{0A} and g_{0P} , and multiply them together to obtain a final, combined estimate: $g_0 = g_{0A} \cdot g_{0P}$.

Our overall approach was to perform this correction on a per-observation basis, to have the flexibility to account for many factors such as platform type, surveyor institution, group size, group composition (e.g. singleton, mother-calf pair, or surface active group), and geographic location (e.g. feeding grounds vs. calving grounds). The level of complexity of the corrections varied by species according to the amount of information available, with North Atlantic right whale having the most elaborate corrections, derived from a substantial set of publications documenting its behavior, and various lesser known odontocetes having corrections based only on platform type (aerial or shipboard), derived from comparatively sparse information. Here we document the corrections used for unidentified beaked whales.

3.1 Aerial Surveys

Palka et al. (2021) developed perception bias corrections using two team, mark recapture distance sampling (MRDS) methodology (Burt et al. 2014) for aerial surveys conducted in 2010-2017 by NOAA NEFSC and SEFSC during the AMAPPS program. These were the only extant perception bias estimates developed from aerial surveys used in our analysis, aside from estimates developed earlier by Palka and colleagues (Palka 2006; Palka et al. 2017). Those earlier efforts utilized older methods and less data than their 2021 analysis, so we applied the Palka et al. (2021) estimates to all aerial survey programs (Table 9).

We applied Palka’s estimate for NEFSC to all programs other than SEFSC on the basis that those programs employed a similar visual scanning protocol that allowed observers to scan from the trackline up to the horizon, while SEFSC’s protocol generally limited scanning only up to 50° from the trackline, resulting in a smaller effective strip width.

We caution that it is possible that perception bias was different on the other aerial programs, as they often used different aircraft, flew at different altitudes, and were staffed by different personnel. Of particular concern are that many programs flew Cessna 337 Skymasters, which had flat windows, while NOAA flew de Havilland Twin Otters, which had bubble windows, which likely afforded a better view of the transect line and therefore might have required less of a correction than the Skymasters. Correcting the other programs using NOAA’s estimate as we have done is likely to yield less bias than leaving them uncorrected, but we urge all programs to undertake their own efforts to estimate perception bias, as resources allow.

We estimated availability bias corrections using the Laake et al. (1997) estimator and dive intervals reported by Palka et al. (2021) and by Barlow (1999) (Table 10). To estimate time in view, needed by the Laake estimator, we used results reported by Robertson et al. (2015), rescaled linearly for each survey program according to its target altitude and speed. We computed availability bias corrections for a single individual of the Mesoplodont guild (Barlow 1999) and Cuvier’s beaked whale (Palka et al. 2021). We then averaged the availability corrections. We believed this to be an adequate way to represent Unidentified beaked whales in our analysis.

We caution that Robertson’s analysis was done for a de Havilland Twin Otter, which may have a different field of view than that of the other aircraft used here, which mainly comprised Cessna 337 Skymasters with flat windows but also a Partenavia P-68 with bubble windows (on the NYS-DEC/TT surveys). However, we note that McLellan et al. (2018) conducted a sensitivity analysis on the influence of the length of the “window of opportunity” to view beaked whales from a Cessna Skymaster on their final density estimates and found that they varied by only a few thousandths of an animal per kilometer when the window of opportunity more than doubled. Still, we urge additional program-specific research into estimation of availability bias.

To address the influence of group size on availability bias, we applied the group availability estimator of McLellan et al. (2018) on a per-observation basis. Following Palka et al. (2021), who also used that method, we assumed that individuals in the group dived asynchronously. The resulting g_{0A} corrections ranged from about 0.1 to 0.45 (Figure 19). We caution that the assumption of asynchronous diving can lead to an underestimation of density and abundance if diving is actually synchronous; see McLellan et al. (2018) for an exploration of this effect. However, if future research finds that this species conducts synchronous dives and characterizes the degree of synchronicity, the model can be updated to account for this knowledge.

Table 9: Perception bias corrections for unidentified beaked whales applied to aerial surveys.

Surveys	Group Size	g_{0P}	g_{0A} Source
SEFSC	Any	0.86	Palka et al. (2021): SEFSC
All others	Any	0.62	Palka et al. (2021): NEFSC

Table 10: Surface and dive intervals for unidentified beaked whales used to estimate availability bias corrections.

Species	Surface Interval (s)	Dive Interval (s)	Source
Cuvier’s beaked whale	426	2060.4	Palka et al. (2021)
Mesoplodon sp.	150	1224.0	Barlow et al. 1999

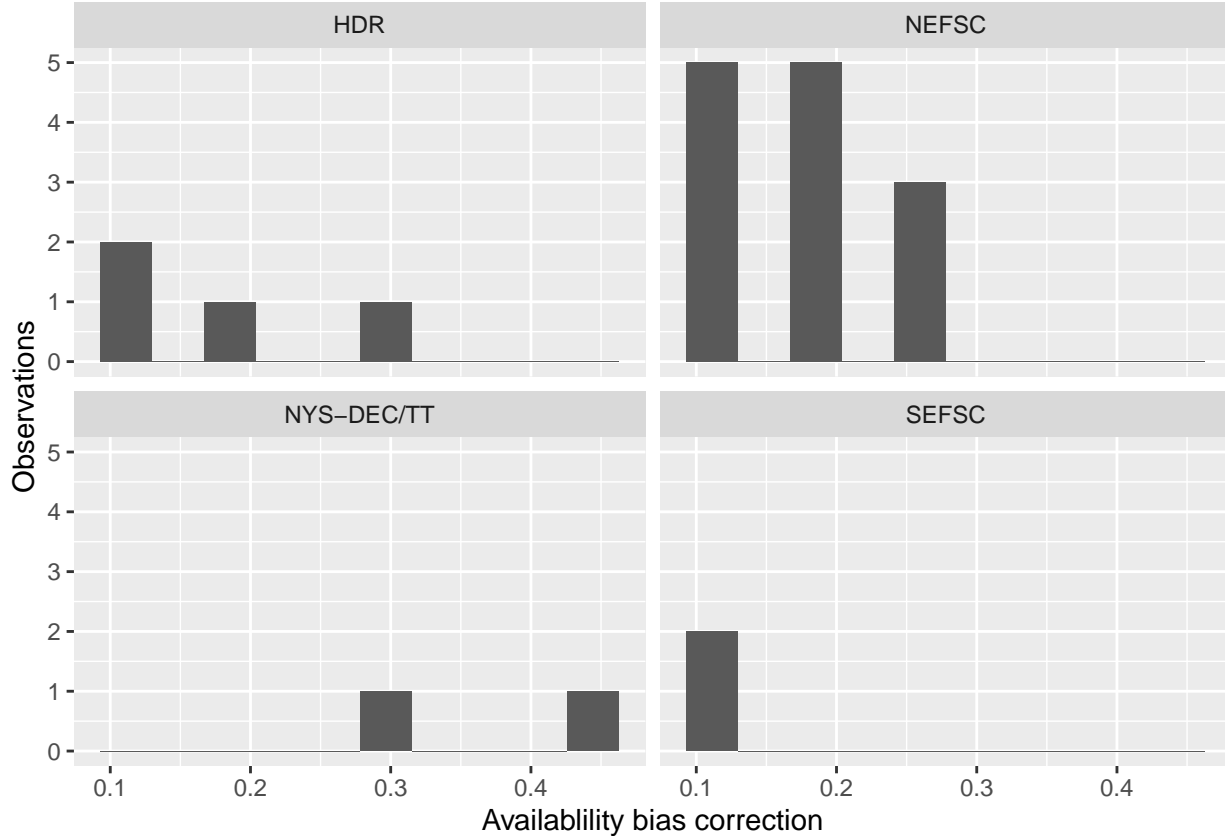


Figure 19: Availability bias corrections for unidentified beaked whales for aerial surveys, by institution.

3.2 Shipboard Surveys

All of the shipboard surveys by this model used high-power (25x150), pedestal-mounted binoculars. Similar to aerial surveys, Palka et al. (2021) developed perception bias corrections using two team, MRDS methodology (Burt et al. 2014) for high-power binocular surveys conducted in 2010-2017 by NOAA NEFSC and SEFSC during the AMAPPS program. These were the only extant perception bias estimates developed from high-power binocular surveys used in our analysis, aside from estimates developed earlier by Palka and colleagues (Palka 2006; Palka et al. 2017). Those earlier efforts utilized older methods and less data than their 2021 analysis, so we applied the Palka et al. (2021) estimates to all shipboard surveys that searched with high-power binoculars (Table 11). Availability bias was calculated as the mean of the Barlow (1999) and Palka et al. (2021) estimates for the Mesoplodont guild and Cuvier’s beaked whales, respectively.

There were no naked eye surveys for Unidentified beaked whales used in this analysis and there were not any Unidentified beaked whales on the Song of the Whale 2019 USA passive acoustic monitoring (PAM) survey (all beaked whales were identified to species) so we excluded it from this model.

Table 11: Perception and availability bias corrections for unidentified beaked whales applied to shipboard surveys.

Surveys	Searching Method	Group Size	g_{0P}	g_{0P} Source	g_{0A}	g_{0A} Source
NEFSC	Binoculars	Any	0.42	Palka et al. (2021): NEFSC	0.84	Palka et al. (2021) and Barlow (1999)
SEFSC	Binoculars	Any	0.32	Palka et al. (2021): SEFSC	0.84	Palka et al. (2021) and Barlow (1999)

4 Density Model

There were enough completely ambiguous sightings (“unidentified beaked whale”) that we could not simply ignore them without biasing composite density of beaked whales low by an unknown but substantial factor. As such, we built a model from the “unidentified beaked whale” sightings. The unidentified beaked whale guild includes both *Ziphius* and *Mesoplodon* species and inherently the model reflects detectability issues given the increased effort and ability to identify beaked whales to the species level in recent years. For example, for the AMAPPS surveys, NMFS NEFSC and SEFSC undertook a concerted effort to boost the taxonomic precision of beaked whale sightings relative to prior surveys (D. Palka, pers. comm.). Separately, the University of North Carolina, Wilmington (UNCW) team led by W. McLellan revisited all beaked whale sightings they collected since 2010 to try to fully identify them from photographs taken of each sighted group. As with the other beaked whale models we chose to fit year-round models to the entire study area. Due to the decreased ability to identify to beaked whales to species in the past we excluded surveys prior to 2010 and also excluded 2020 from the models so that we could use micronekton biomass, distance to eddies and kinetic energy covariates as candidates in the models.

Off the U.S. Atlantic coast, unidentified beaked whale observations primarily occurred along the shelf-edge and in deep waters, although there are a few observations on the shelf (Figure 1). The survey segments with observations used in this study occurred between 52 m to 5115 m depth, with only 15 observations occurring in waters shallower than 900 m. Ziphiidae species are comprised of both Cuvier’s and Mesoplodonts and as such, the animals in this guild feed on squid and benthic fish, are deep diving, occur in small groups, are cryptic at the surface and are vocally active during foraging dives. Their habitat preferences include deep waters with depths greater than 1,000 m (Baird et al. 2004) and static bathymetric features such as canyons, seamounts and shelf-edges (Waring et al. 2001; MacLeod et al. 2005; Moulins et al. 2007). These features likely help concentrate prey and thus provide ideal foraging habitat (Baumgartner 1997; Moulins et al. 2007).

The unidentified beaked whale model contained over 766,000 km of segments with 117 total observations. The top model selected with the highest explained deviance and lowest AIC and REML scores was a climatological model. This was a fairly simple model with only four covariates retained in the top model. The covariates included depth, slope, distance to the 1500m isobath, and distance to cyclonic eddies (Table 12) (Figure 23). There was a positive relationship to all covariates. The relationships predicted more animals at deeper depth, higher slope, further from the 1500 m isobath (on the deeper side) and further from cyclonic eddies.

4.1 Final Model

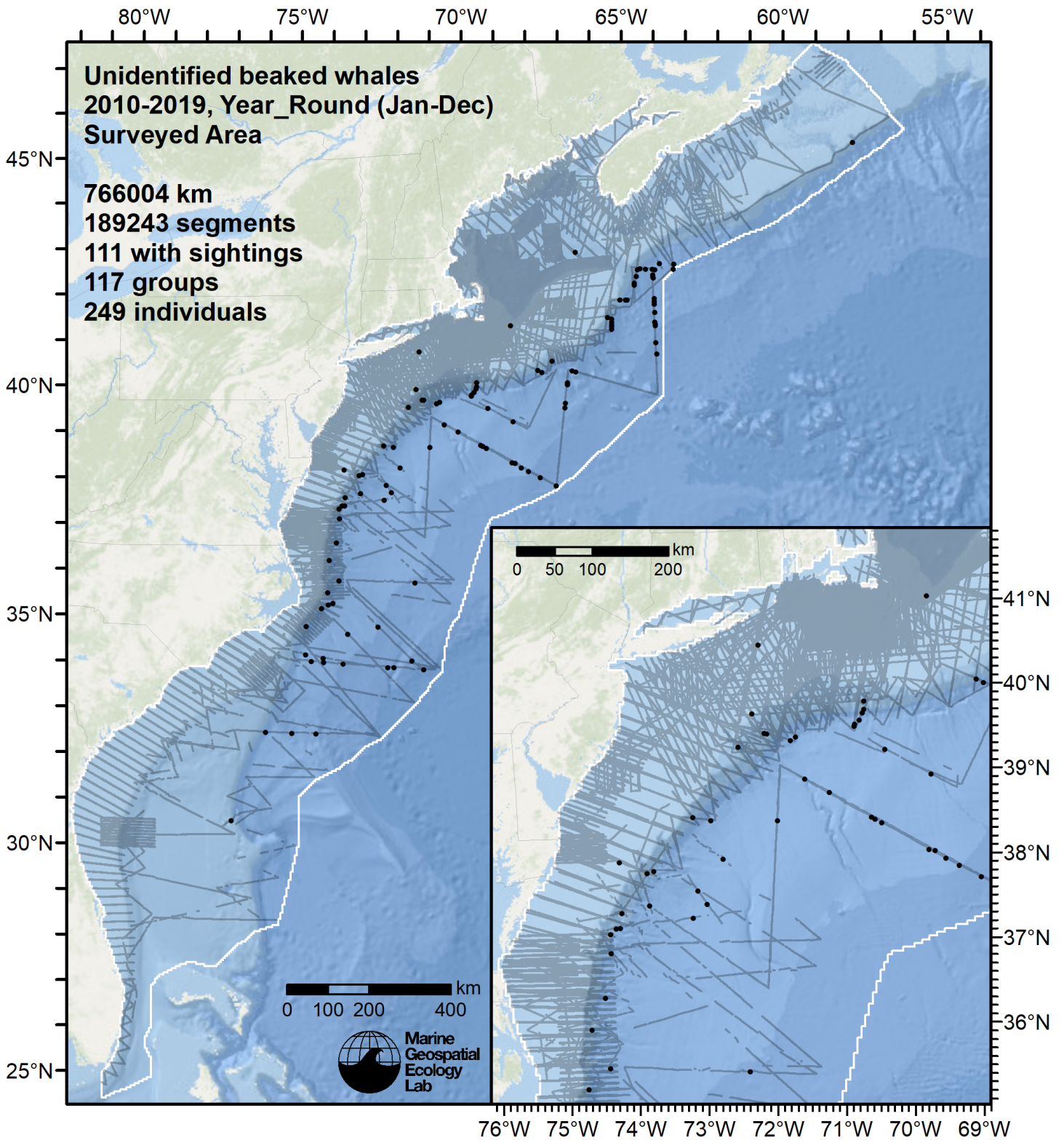


Figure 20: Survey segments used to fit the model. Black points indicate segments with observations.

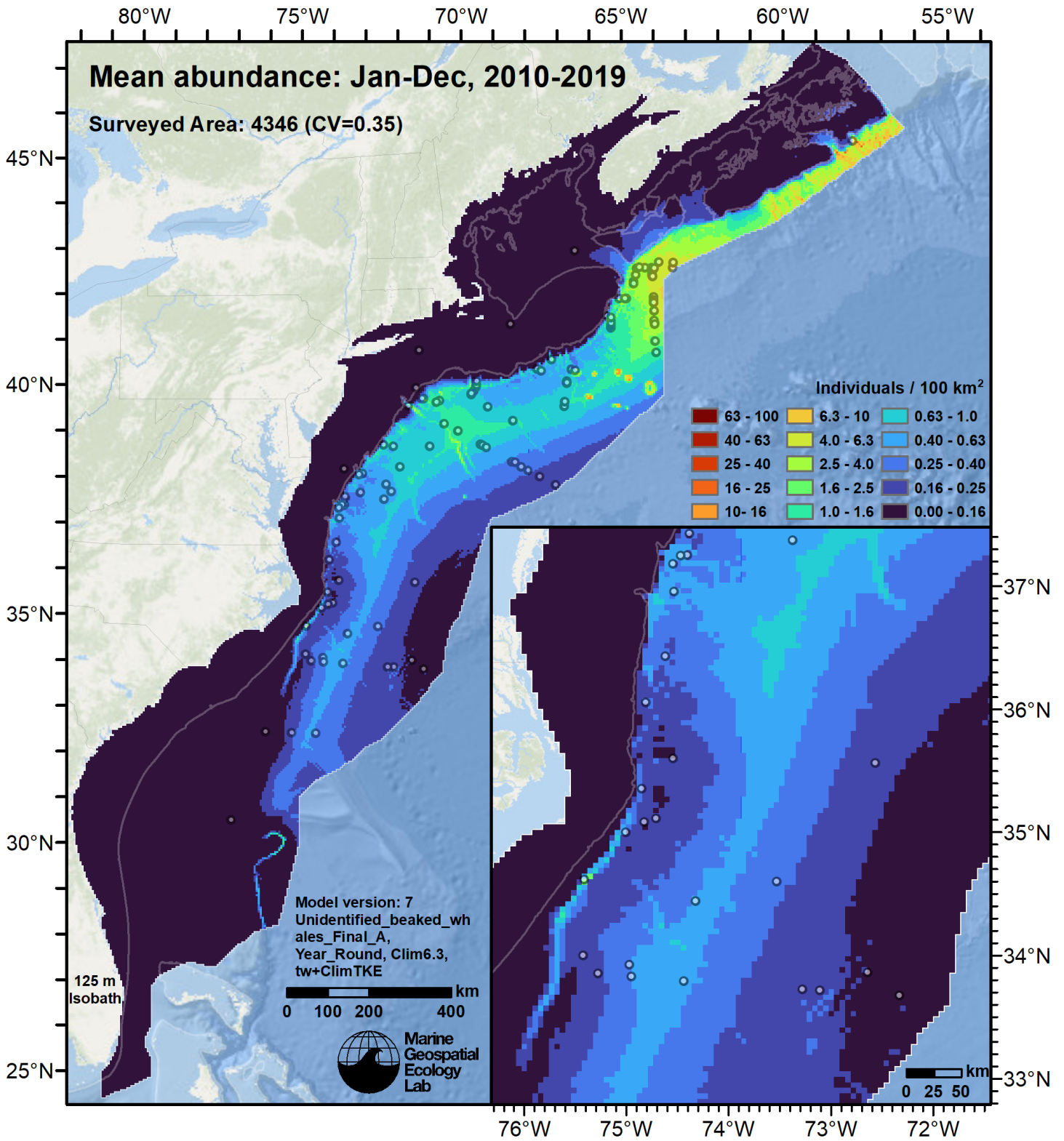


Figure 21: Unidentified beaked whales mean density for the indicated period, as predicted by the model. Open circles indicate segments with observations. Mean total abundance and its coefficient of variation (CV) are given in the subtitle. Variance was estimated with the analytic approach given by Miller et al. (2022), Appendix S1, and accounts both for uncertainty in model parameter estimates and for seasonal variability in dynamic covariates but not interannual variability in them, as these covariates were monthly climatological averages.

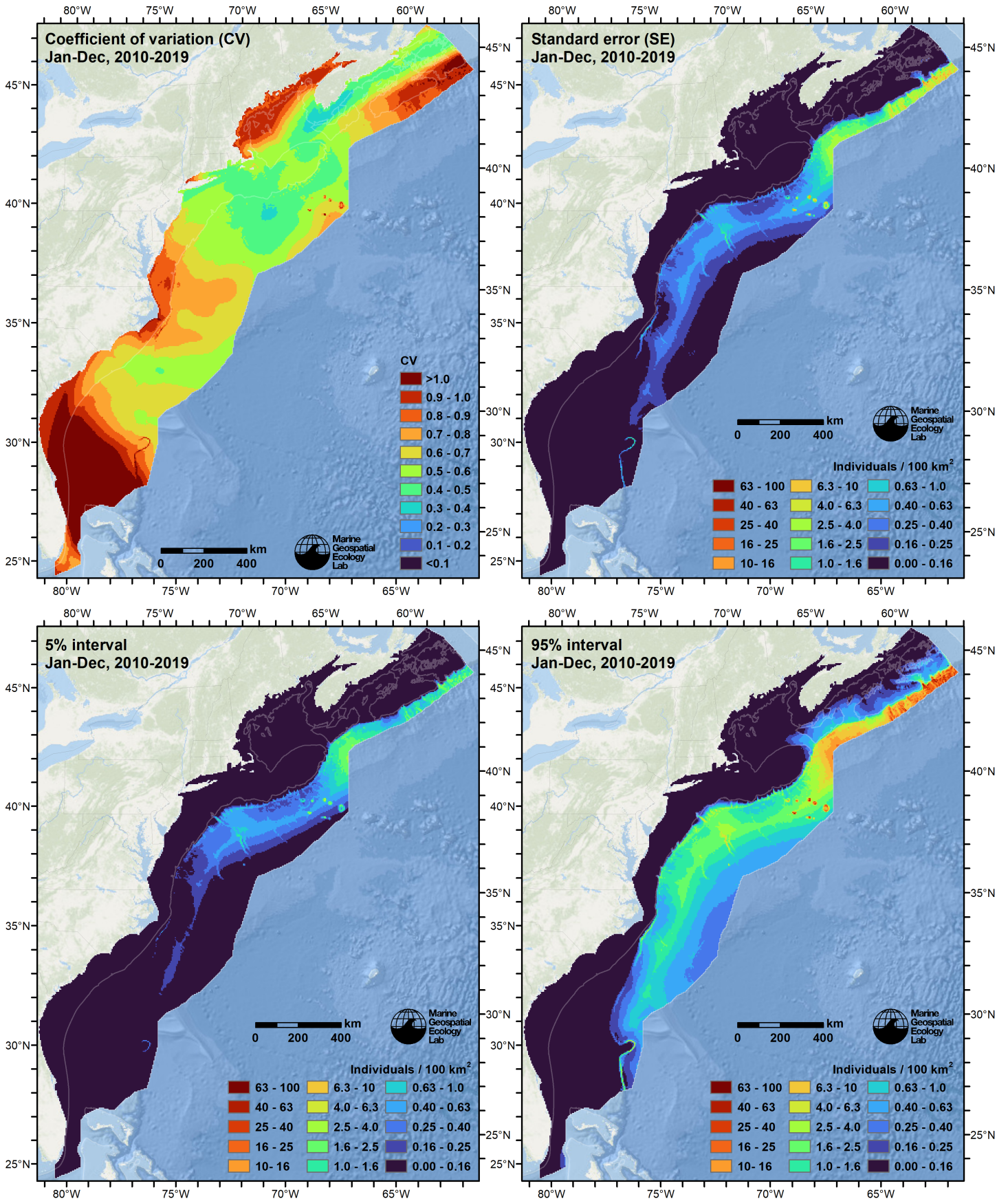


Figure 22: Uncertainty statistics for the unidentified beaked whales mean density surface (Figure 21) predicted by the model. Variance was estimated with the analytic approach given by Miller et al. (2022), Appendix S1, and accounts both for uncertainty in model parameter estimates and for seasonal variability in dynamic covariates but not interannual variability in them, as these covariates were monthly climatological averages.

Statistical output for this model:

Family: Tweedie(p=1.219)

Link function: log

Formula:

```
IndividualsCorrected ~ offset(log(SegmentArea)) + s(log10(pmax(10,
  Depth)), bs = "ts") + s(pmin(Slope, 30), bs = "ts") + s(pmax(-300,
  pmin(I(DistTo1500m/1000), 100)), bs = "ts") + s(pmin(I(ClimDistToCEddy30/1000),
  450), bs = "ts")
```

Parametric coefficients:

	Estimate	Std. Error	t value	Pr(> t)
(Intercept)	-23.9880	0.3549	-67.6	<2e-16 ***

Signif. codes: 0 '***' 0.001 '**' 0.01 '*' 0.05 '.' 0.1 ' ' 1

Approximate significance of smooth terms:

	edf	Ref.df	F	p-value
s(log10(pmax(10, Depth)))	1.1022	9	3.207	< 2e-16 ***
s(pmin(Slope, 30))	0.9552	9	2.070	3.55e-06 ***
s(pmax(-300, pmin(I(DistTo1500m/1000), 100)))	1.5134	9	6.656	< 2e-16 ***
s(pmin(I(ClimDistToCEddy30/1000), 450))	1.4893	9	11.508	< 2e-16 ***

Signif. codes: 0 '***' 0.001 '**' 0.01 '*' 0.05 '.' 0.1 ' ' 1

R-sq.(adj) = 0.0282 Deviance explained = 41.1%

-REML = 1016 Scale est. = 20.296 n = 189243

Method: REML Optimizer: outer newton

full convergence after 11 iterations.

Gradient range [-4.620081e-05,3.980274e-05]

(score 1015.951 & scale 20.2955).

Hessian positive definite, eigenvalue range [0.4454398,829.1341].

Model rank = 37 / 37

Basis dimension (k) checking results. Low p-value (k-index<1) may indicate that k is too low, especially if edf is close to k'.

	k'	edf	k-index	p-value
s(log10(pmax(10, Depth)))	9.000	1.102	0.85	0.005 **
s(pmin(Slope, 30))	9.000	0.955	0.89	<2e-16 ***
s(pmax(-300, pmin(I(DistTo1500m/1000), 100)))	9.000	1.513	0.86	<2e-16 ***
s(pmin(I(ClimDistToCEddy30/1000), 450))	9.000	1.489	0.90	0.005 **

Signif. codes: 0 '***' 0.001 '**' 0.01 '*' 0.05 '.' 0.1 ' ' 1

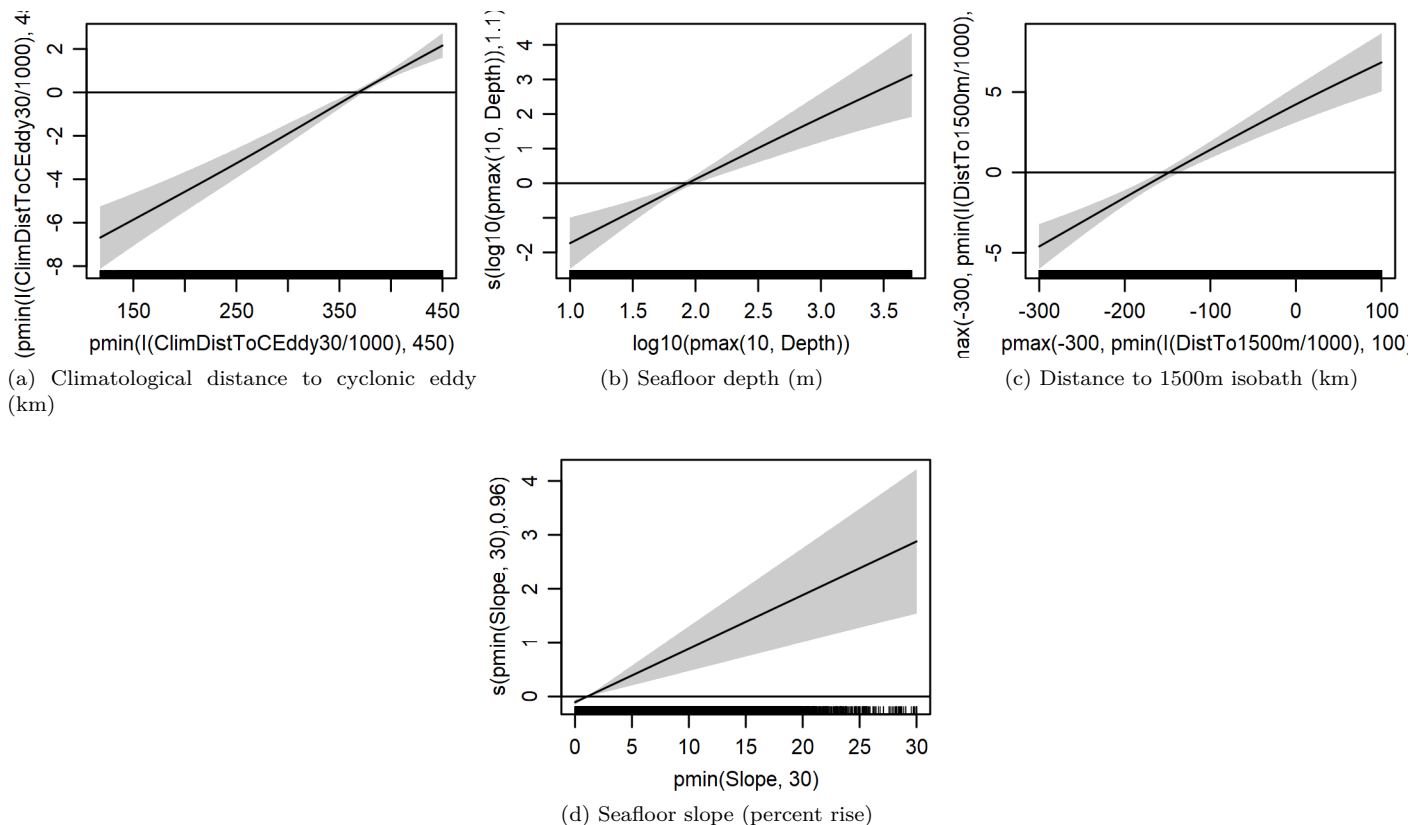


Figure 23: Functional plots for the final model. Transforms and other treatments are indicated in axis labels. \log_{10} indicates the covariate was \log_{10} transformed. $pmax$ and $pmin$ indicate the covariate’s minimum and maximum values, respectively, were Winsorized to the values shown. Winsorization was used to prevent runaway extrapolations during prediction when covariates exceeded sampled ranges, or for ecological reasons, depending on the covariate. $/1000$ indicates meters were transformed to kilometers for interpretation convenience.

Table 12: Covariates used in the final model.

Covariate	Description
ClimDistToCEddy30	Climatological monthly mean distance (km) to the edge of the closest cyclonic mesoscale eddy at least 30 days old, derived with MGET (Roberts et al. (2010)) from the Aviso Mesoscale Eddy Trajectories Atlas (META2.0), produced by SSALTO/DUACS and distributed by AVISO+ (https://aviso.altimetry.fr) with support from CNES, in collaboration with Oregon State University with support from NASA, using the method of Schlax and Chelton (2016), based on Chelton et al. (2011)
Depth	Depth (m) of the seafloor, from SRTM30_PLUS (Becker et al. (2009))
DistTo1500m	Distance (km) to the 1500m isobath, derived from SRTM30_PLUS (Becker et al. (2009))
Slope	Slope (percent rise) of the seafloor, derived from SRTM30_PLUS (Becker et al. (2009))

4.2 Diagnostic Plots

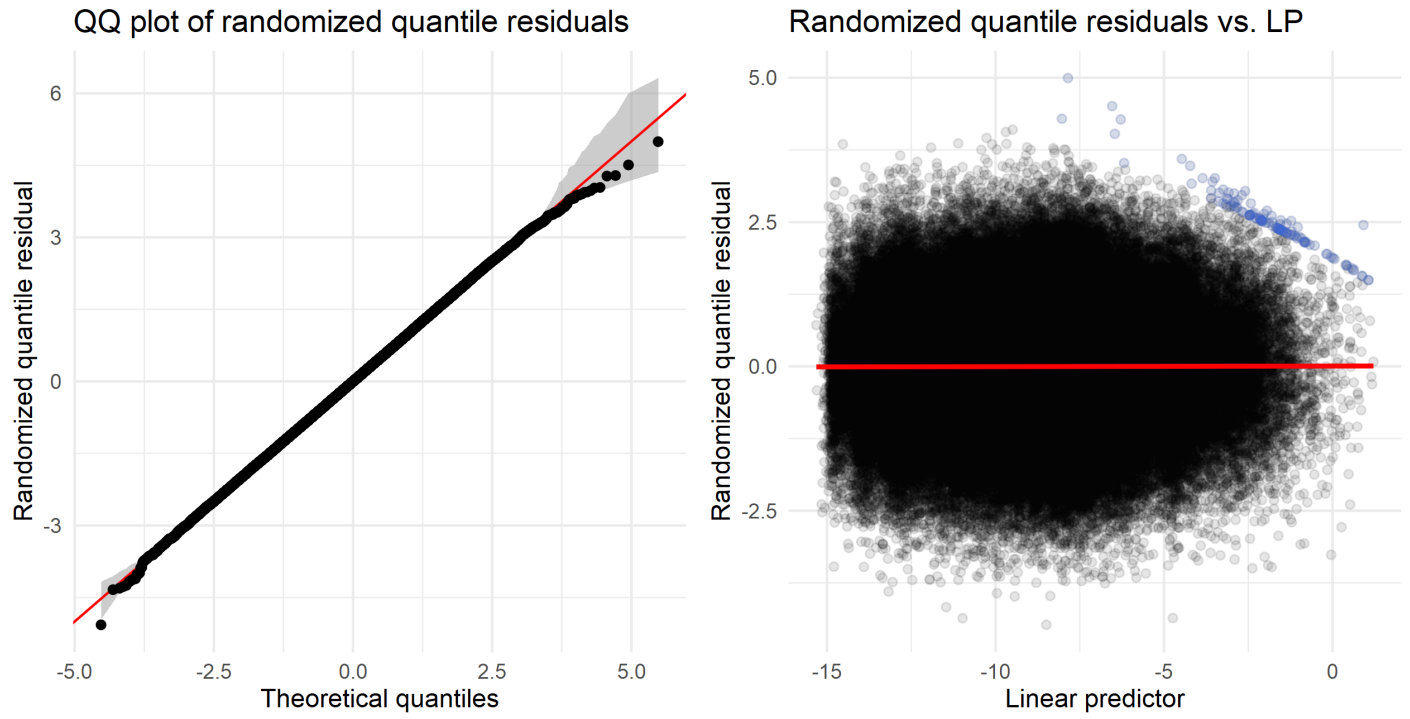


Figure 24: Residual plots for the final model.

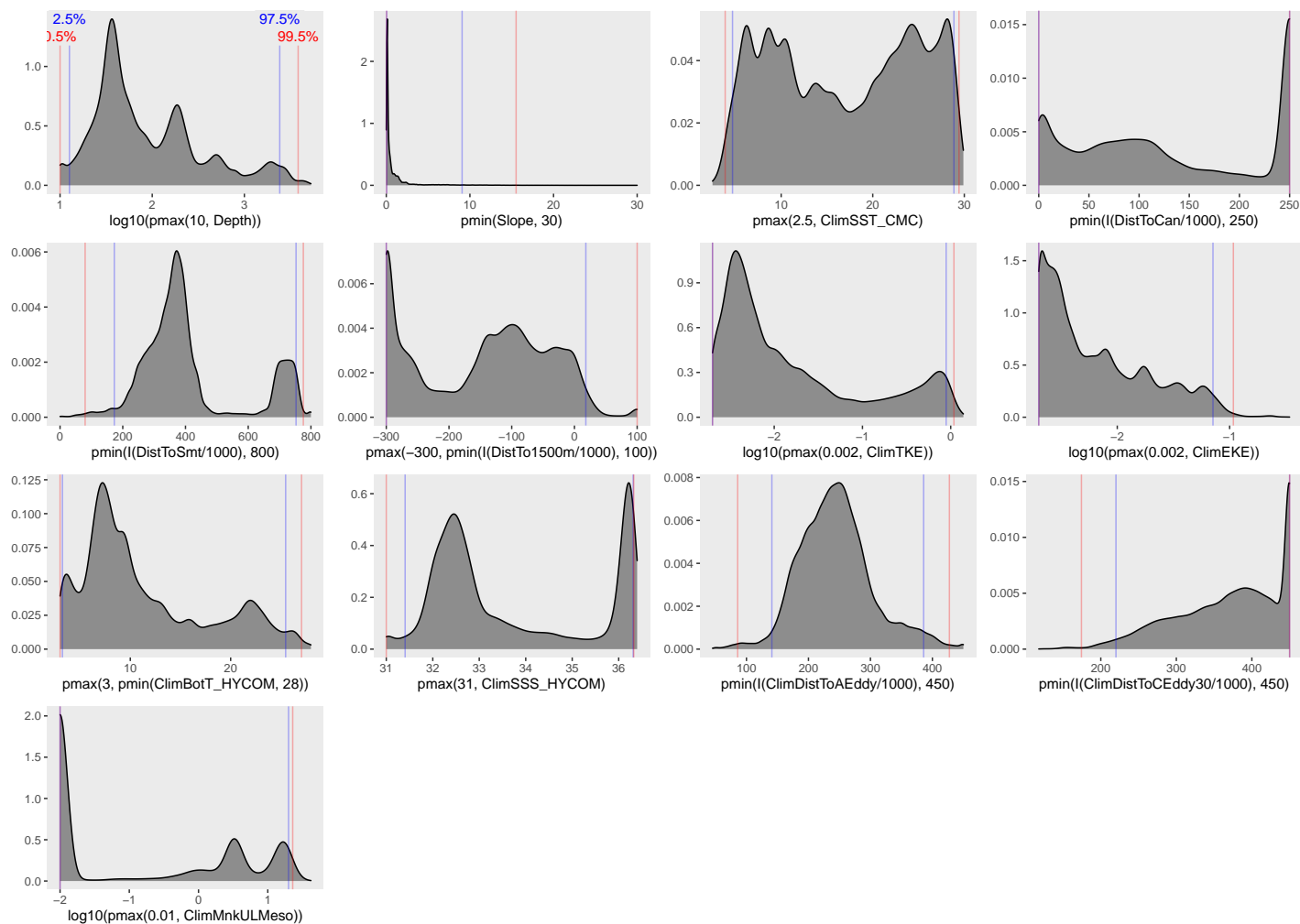


Figure 25: Density histograms showing the distributions of the covariates considered during the final model selection step. The final model may have included only a subset of the covariates shown here (see Figure 23), and additional covariates may have been considered in preceding selection steps. Red and blue lines enclose 99% and 95% of the distributions, respectively. Transforms and other treatments are indicated in axis labels. \log_{10} indicates the covariate was \log_{10} transformed. $pmax$ and $pmin$ indicate the covariate's minimum and maximum values, respectively, were Winsorized to the values shown. Winsorization was used to prevent runaway extrapolations during prediction when covariates exceeded sampled ranges, or for ecological reasons, depending on the covariate. $/1000$ indicates meters were transformed to kilometers for interpretation convenience.

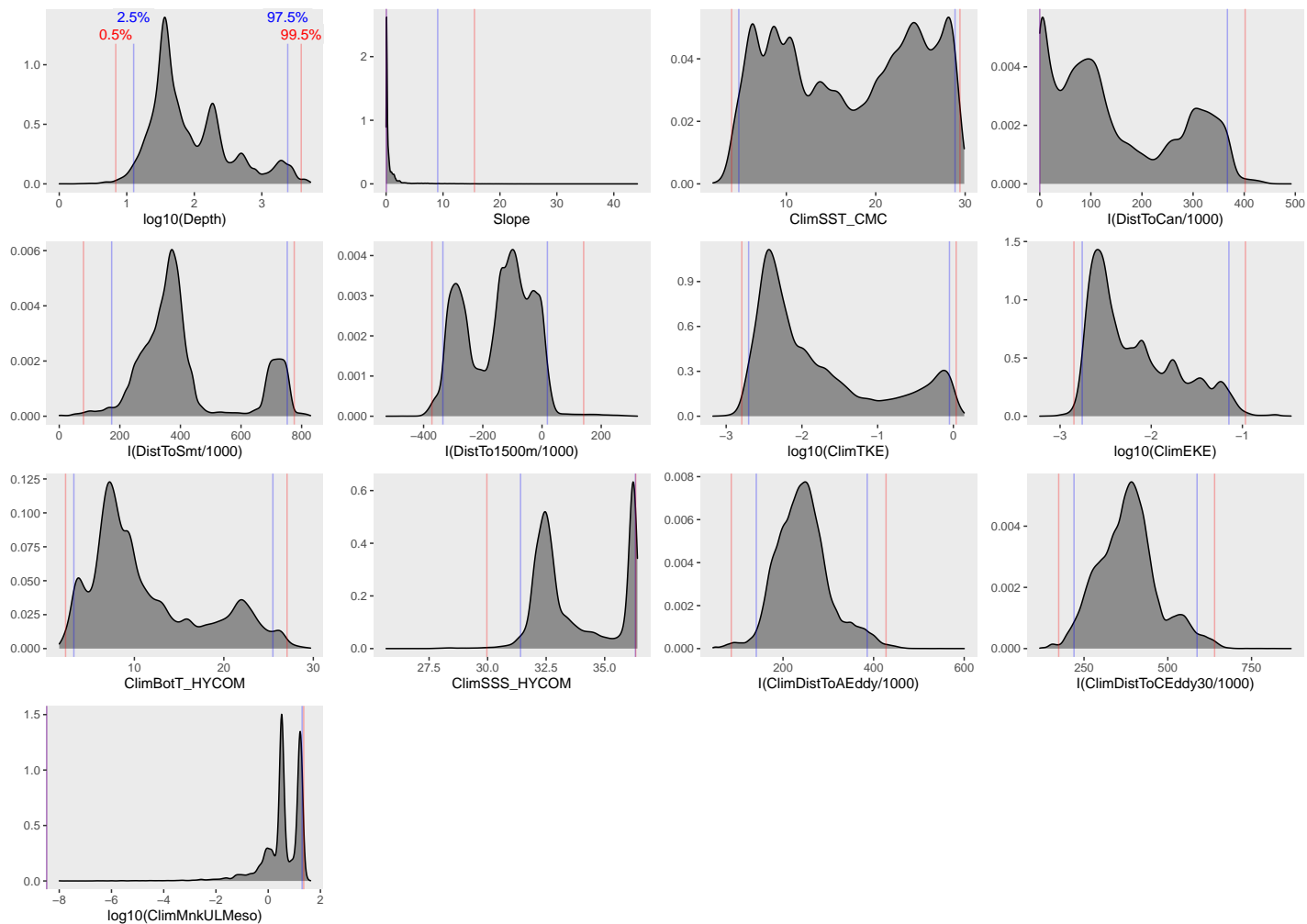


Figure 26: Density histograms shown in Figure 25 replotted without Winsorization, to show the full range of sampling represented by survey segments.

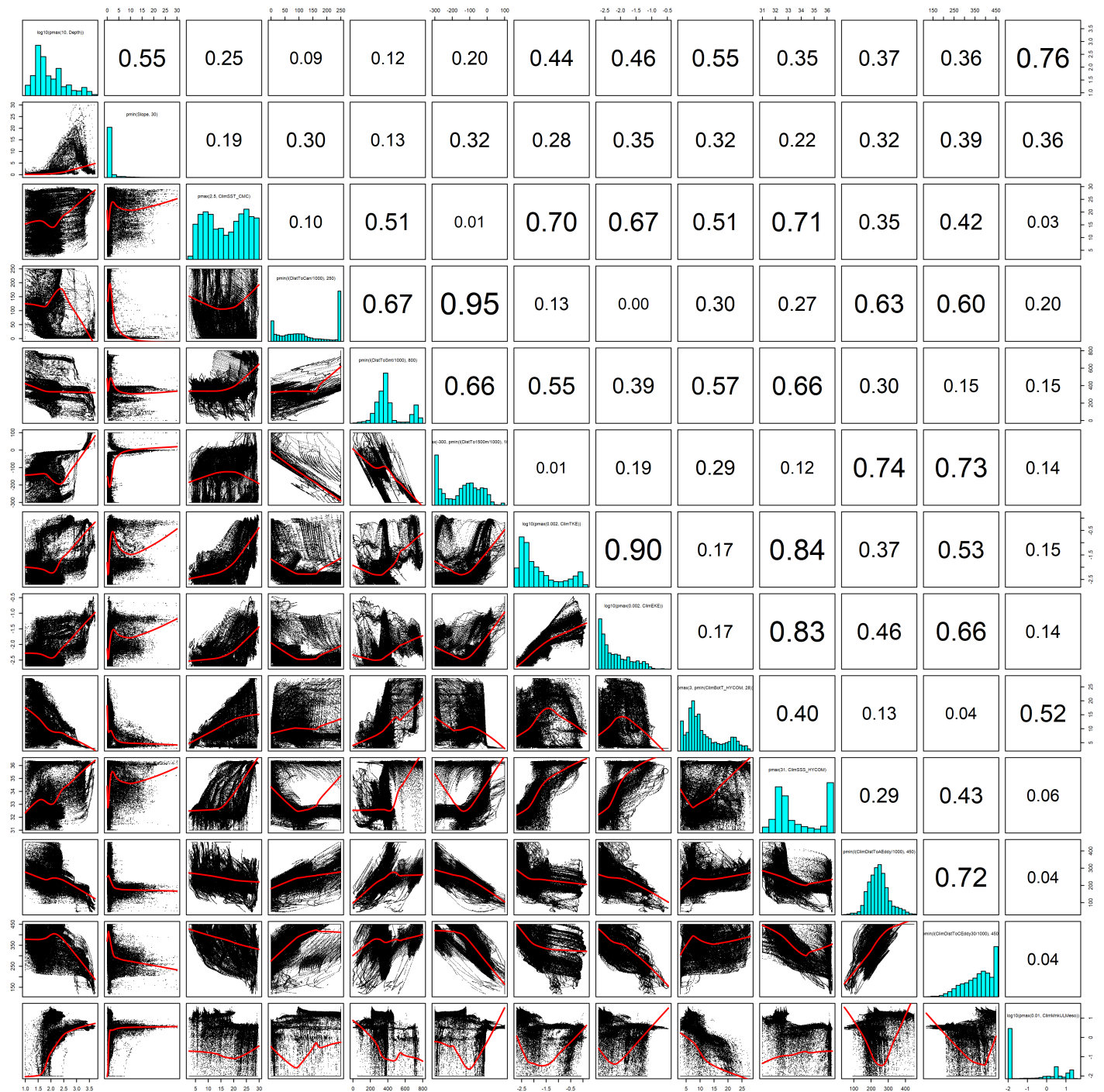


Figure 27: Scatterplot matrix of the covariates considered during the final model selection step. The final model may have included only a subset of the covariates shown here (see Figure 23), and additional covariates may have been considered in preceding selection steps. Covariates are transformed and Winsorized as shown in Figure 25. This plot is used to check simple correlations between covariates (via pairwise Pearson coefficients above the diagonal) and visually inspect for concurvity (via scatterplots and red lowess curves below the diagonal).

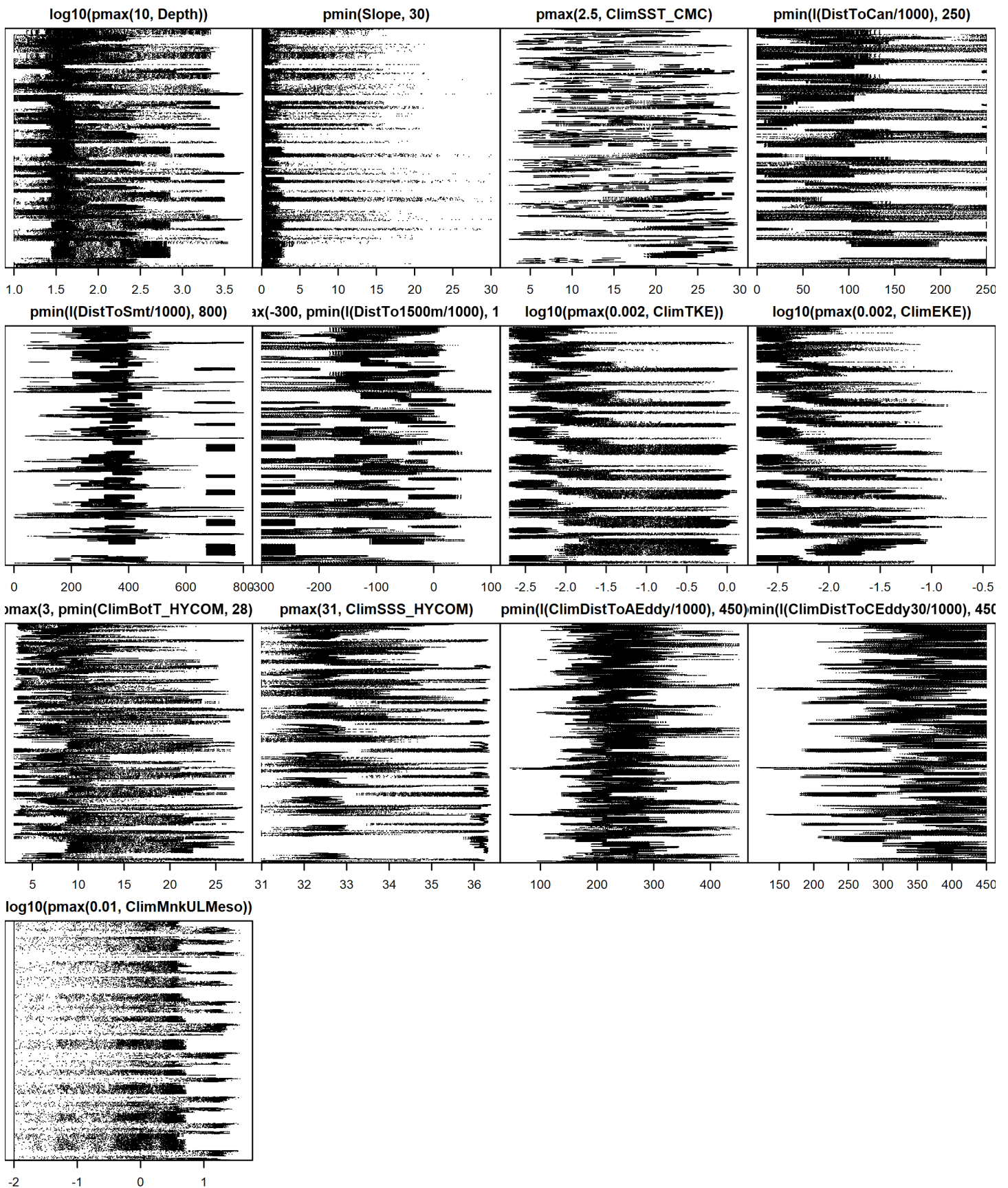


Figure 28: Dotplot of the covariates considered during the final model selection step. The final model may have included only a subset of the covariates shown here (see Figure 23), and additional covariates may have been considered in preceding selection steps. Covariates are transformed and Winsorized as shown in Figure 25. This plot is used to check for suspicious patterns and outliers in the data. Points are ordered vertically by segment ID, sequentially in time.

4.3 Extrapolation Diagnostics

4.3.1 Univariate Extrapolation

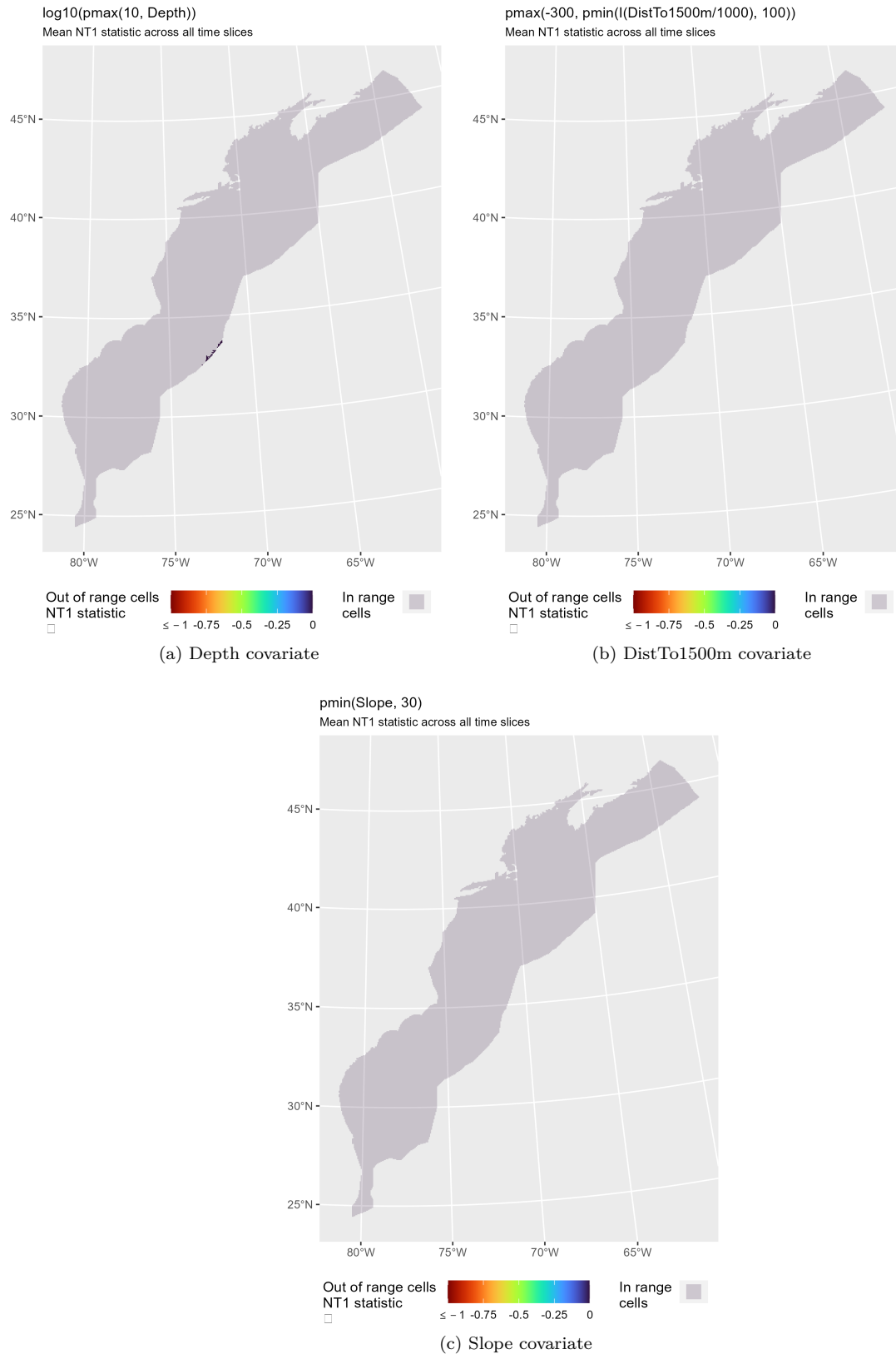


Figure 29: NT1 statistic (Mesgaran et al. (2014)) for static covariates used in the model. Areas outside the sampled range of a covariate appear in color, indicating univariate extrapolation of that covariate occurred there. Areas within the sampled range appear in gray, indicating it did not occur.

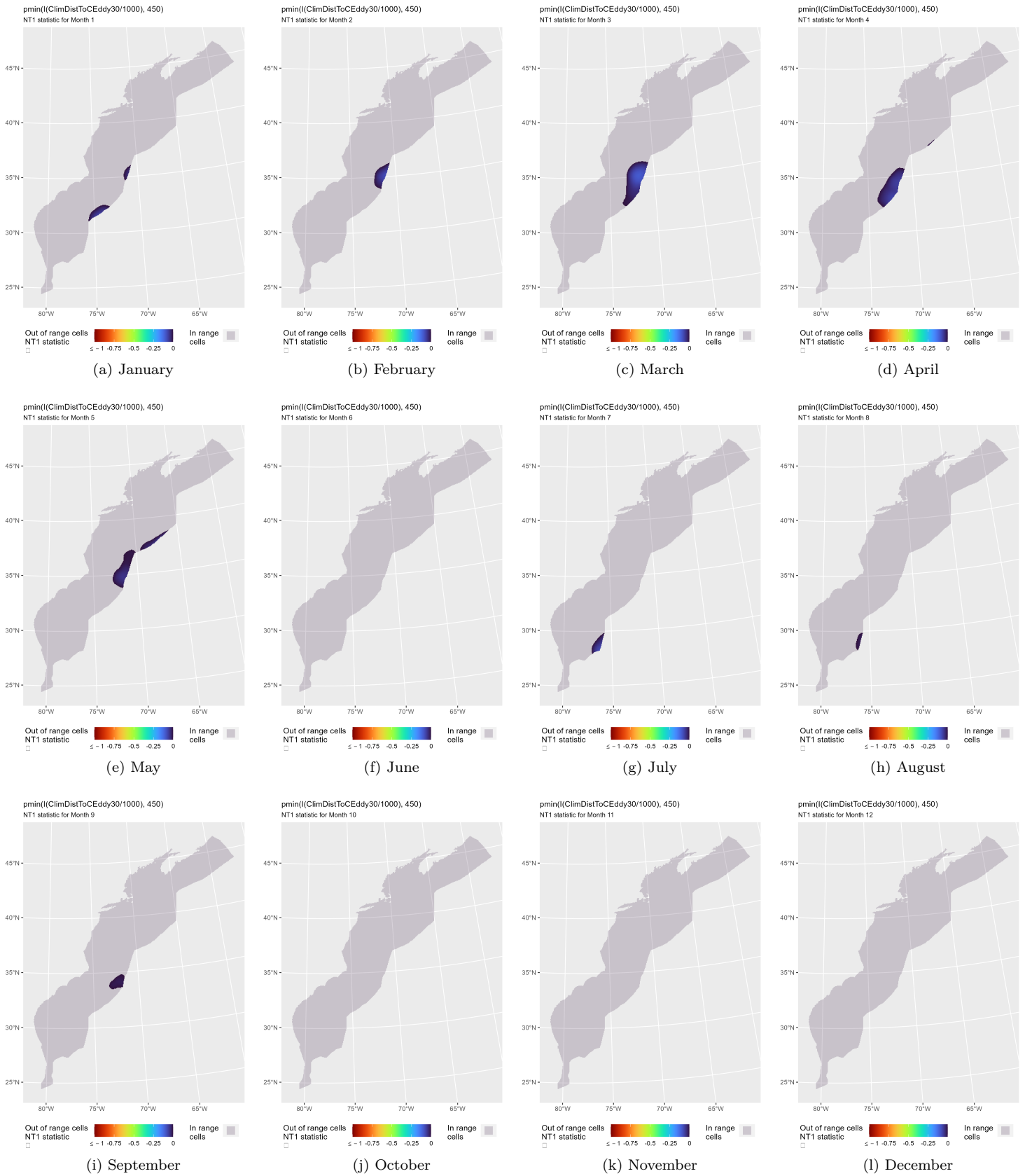


Figure 30: NT1 statistic (Mesgaran et al. (2014)) for the ClimDistToCEddy30 covariate in the model. Areas outside the sampled range of a covariate appear in color, indicating univariate extrapolation of that covariate occurred there during the month. Areas within the sampled range appear in gray, indicating it did not occur.

4.3.2 Multivariate Extrapolation

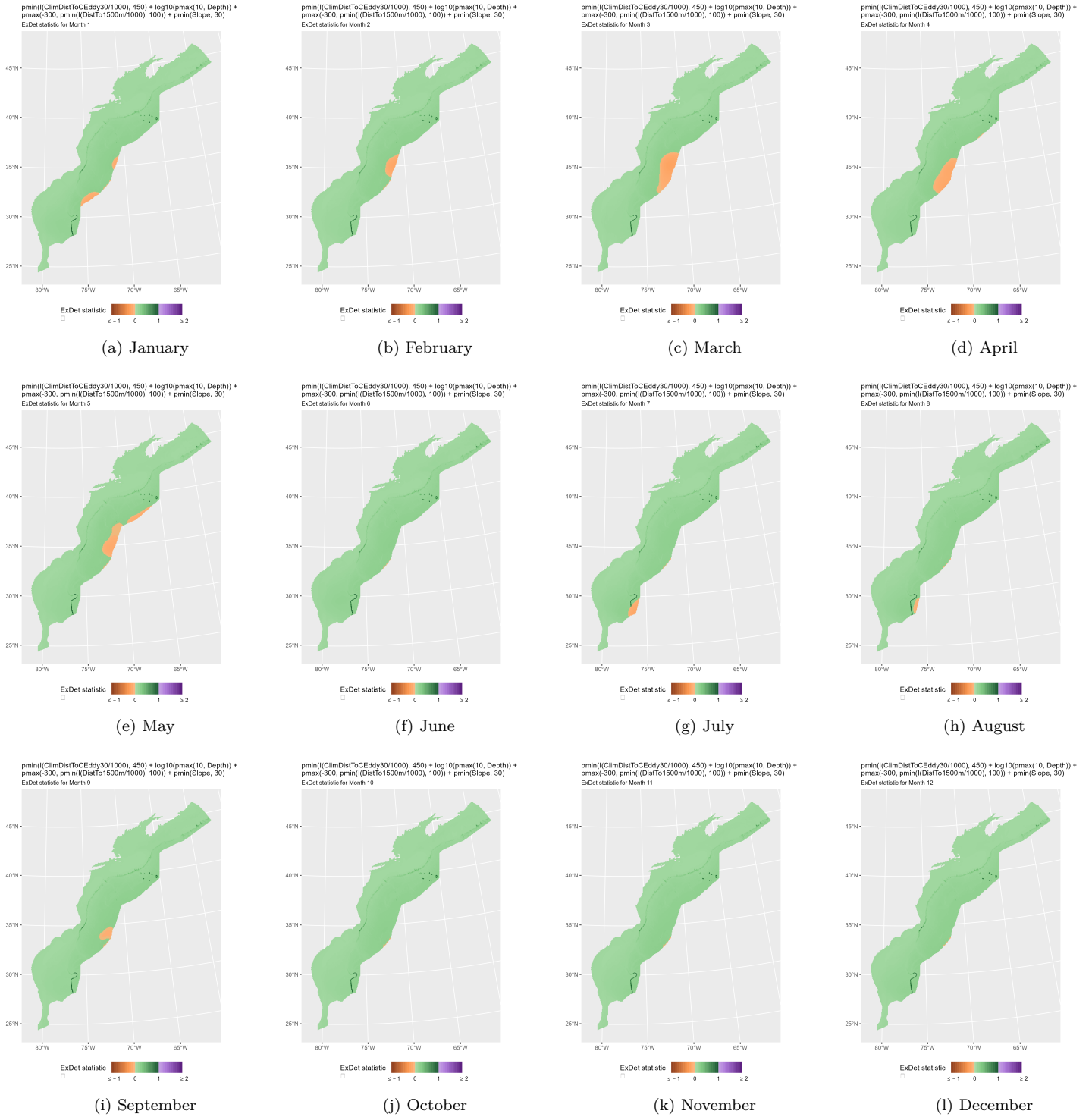


Figure 31: ExDet statistic (Mesgaran et al. (2014)) for all of the covariates used in the model. Areas in orange ($\text{ExDet} < 0$) required univariate extrapolation of one or more covariates (see previous section). Areas in purple ($\text{ExDet} > 1$), did not require univariate extrapolation but did require multivariate extrapolation, by virtue of having novel combinations of covariates not represented in the survey data, according to the NT2 statistic (Mesgaran et al. (2014)). Areas in green ($0 \geq \text{ExDet} \leq 1$) did not require either type of extrapolation.

5 Predictions

Based on our evaluation of this model in the context of what is known of this species (see Section 4), we summarized its predictions into single, year-round climatological density and uncertainty surfaces (Figure 33). To illustrate the seasonal dynamics that result when predictions are summarized monthly instead, we included monthly mean abundances (Figure 32, Table 13), but to avoid confusion we did not include monthly maps in this report. They are available from us on request, but we recommend the year-round map be used for decision-making purposes, as discussed in Section 6.

5.1 Summarized Predictions

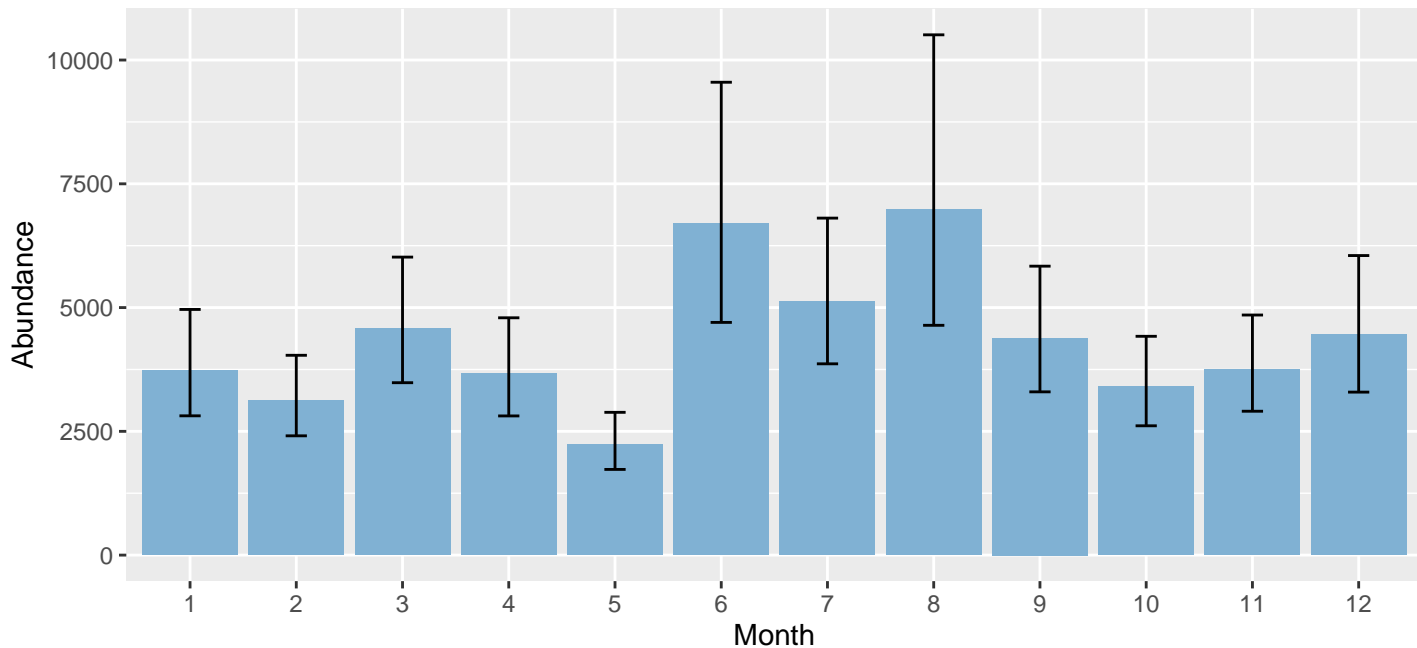


Figure 32: Mean monthly abundance for the prediction area for 2010-2019. Error bars are a 95% interval, made with a log-normal approximation using the prediction’s CV. The CV was estimated with the analytic approach given by Miller et al. (2022), Appendix S1, and accounts both for uncertainty in model parameter estimates and for temporal variability in dynamic covariates.

Table 13: Mean monthly abundance and density for the prediction area for 2010-2019. CV and intervals estimated as described for the previous figure.

Month	Abundance	CV	95% Interval	Area (km ²)	Density (individuals / 100 km ²)
1	3,736	0.146	2,814 - 4,962	1,272,925	0.294
2	3,119	0.132	2,409 - 4,036	1,272,925	0.245
3	4,579	0.140	3,483 - 6,019	1,272,925	0.360
4	3,671	0.137	2,811 - 4,794	1,272,925	0.288
5	2,234	0.131	1,731 - 2,884	1,272,925	0.176
6	6,701	0.182	4,701 - 9,552	1,272,925	0.526
7	5,129	0.145	3,864 - 6,807	1,272,925	0.403
8	6,984	0.211	4,642 - 10,509	1,272,925	0.549
9	4,387	0.146	3,298 - 5,837	1,272,925	0.345
10	3,398	0.135	2,612 - 4,420	1,272,925	0.267
11	3,754	0.131	2,906 - 4,850	1,272,925	0.295
12	4,464	0.156	3,293 - 6,051	1,272,925	0.351

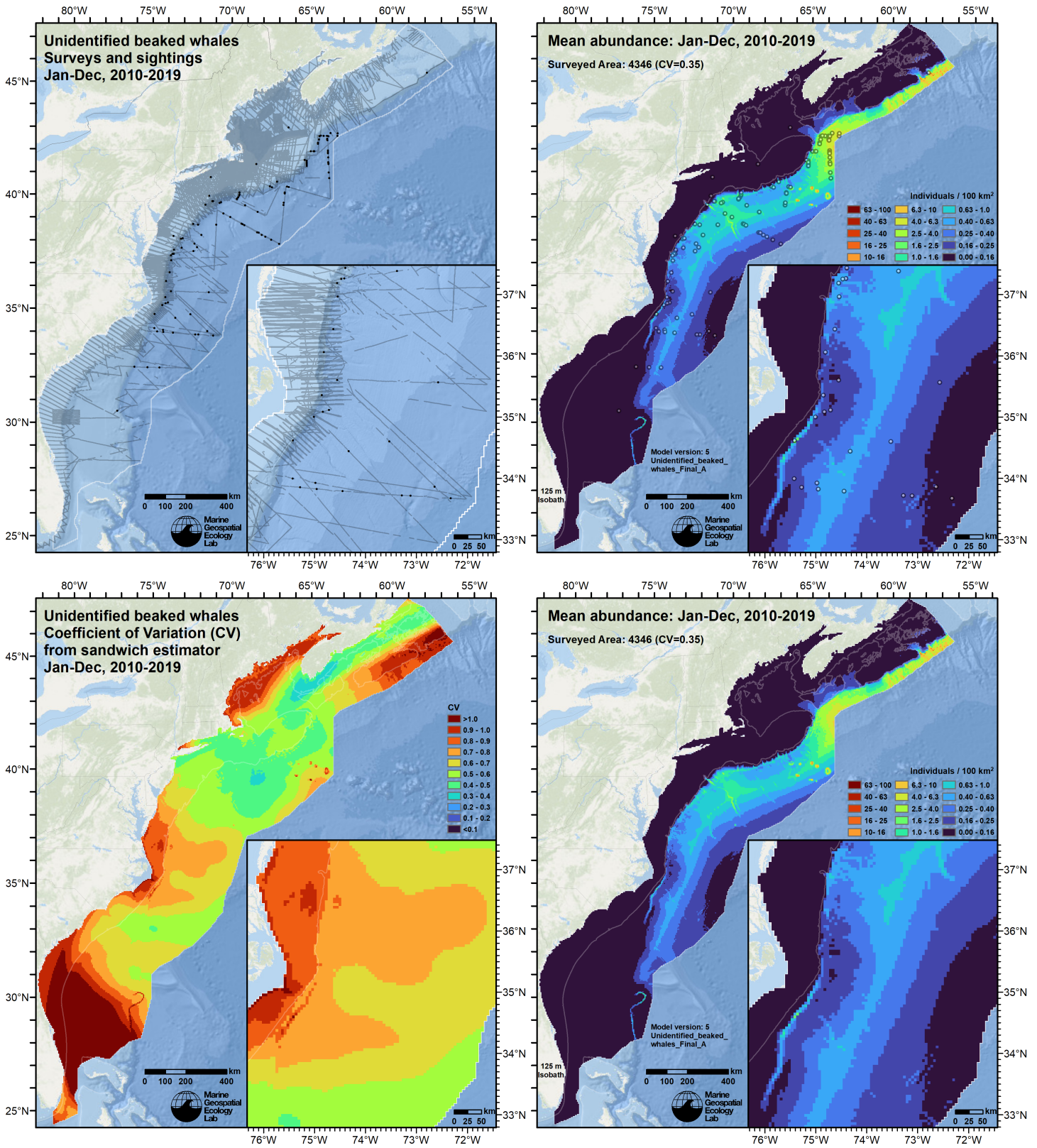


Figure 33: Survey effort and observations (top left), predicted density with observations (top right), predicted density without observations (bottom right), and coefficient of variation of predicted density (bottom left), for the given era. Variance was estimated with the analytic approach given by Miller et al. (2022), Appendix S1, and accounts both for uncertainty in model parameter estimates and for temporal variability in dynamic covariates.

5.2 Abundance Comparisons

5.2.1 NOAA Stock Assessment Report

Table 14: Comparison of regional abundance estimates from the 2019 NOAA Stock Assessment Report (SAR) (Hayes et al. (2020)) to estimates from this density model extracted from roughly comparable zones (Figure 34 below). The SAR estimates were based on a single year of surveying, while the model estimates were taken from the multi-year mean density surfaces we provide to model users (Section 5.1).

2021 Stock Assessment Report			Density Model		
Month/Year	Area	N_{est}	Period	Zone	Abundance
Jun-Sep 2016	Central Virginia to lower Bay of Fundy ^a	3,755	Year-Round 2010-2019	NEFSC	2,010
Jun-Aug 2016	Florida to central Virginia ^b	2,812	Year-Round 2010-2019	SEFSC	645
Jun-Aug 2016	Total	6,567	Year-Round 2010-2019	Total	2,655
	Bay of Fundy/Scotian Shelf		Year-Round 2010-2019	Canada ^c	1,681

^a Estimate originally from Palka (2020).

^b Estimate originally from Garrison (2020).

^c Our Canada zone is roughly comparable to the SAR's Bay of Fundy/Scotian Shelf area (excluding the Gulf of St. Lawrence) however no estimates were provided by the SAR for this region.

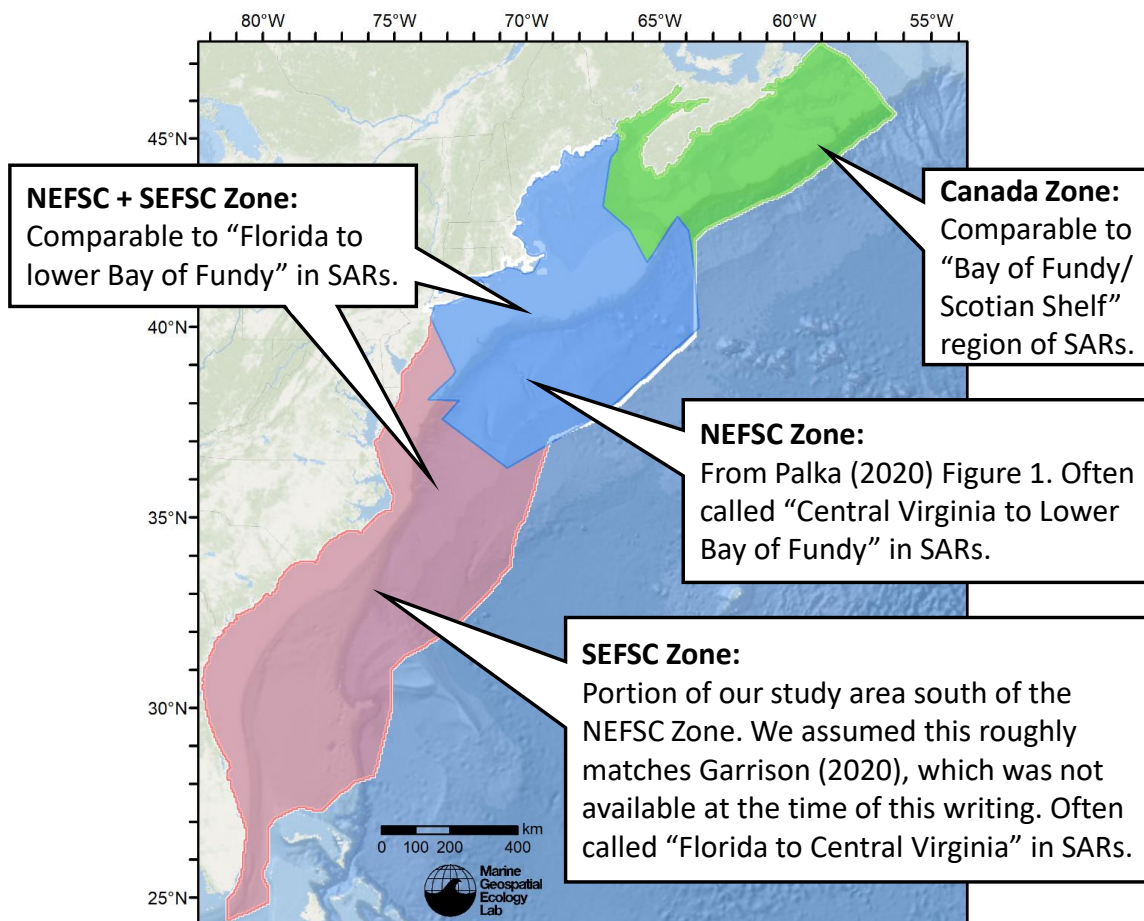


Figure 34: Zones for which we extracted abundance estimates from the density model for comparison to estimates from the NOAA Stock Assessment Report.

5.2.2 Previous Density Model

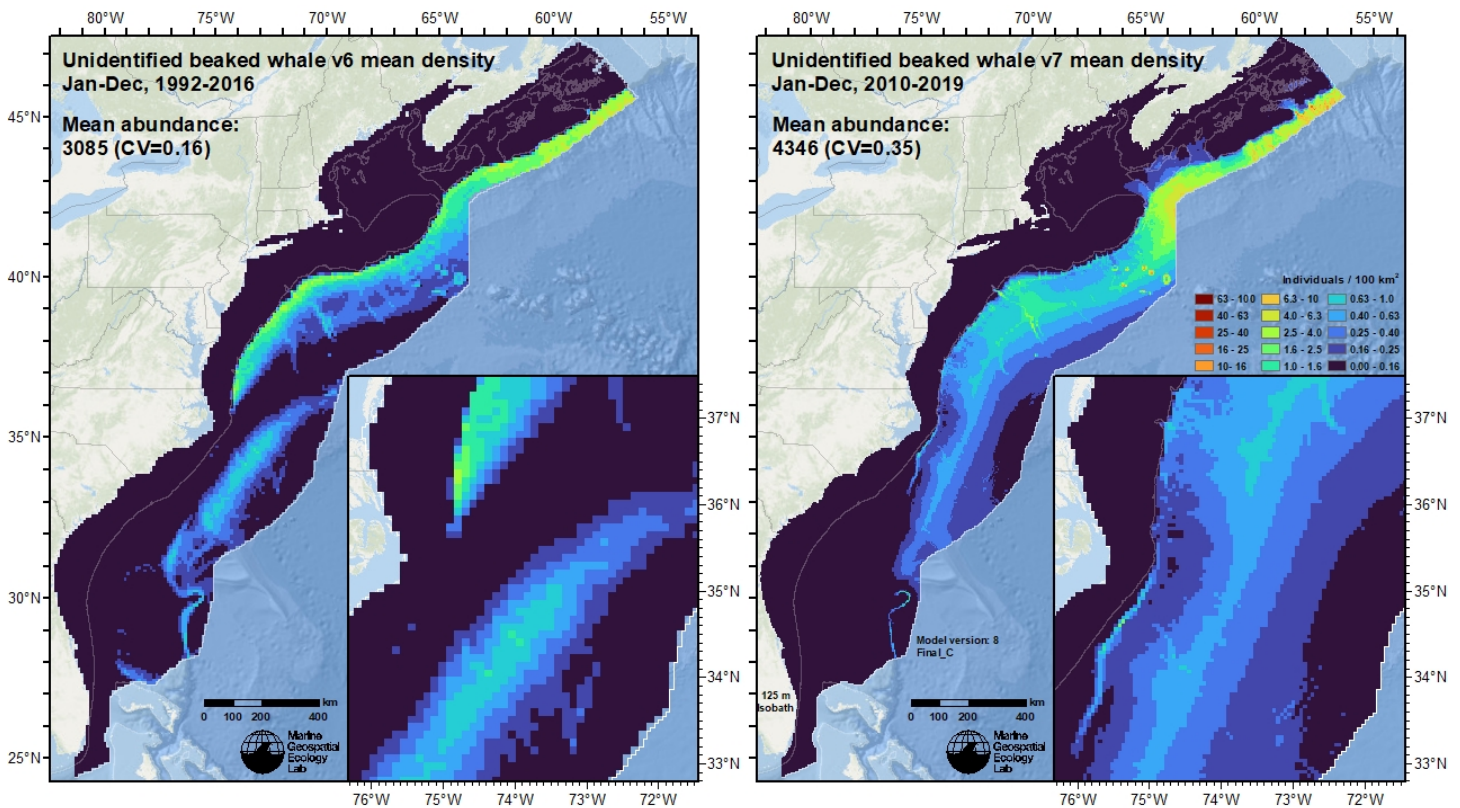


Figure 35: Comparison of the mean density predictions from the previous model (left) released by Roberts et al. (2017) to those from this model (right).

6 Discussion

The mean year-round abundance was 4,346 unidentified beaked whales with highest abundance predicted in the northern portion of the study area. The model reflects both the ecology of beaked whales and the relative success amongst the collaborators in taxonomically identifying beaked whales. For example, the relatively low density around the Cape Hatteras area, a location where many beaked whales are present, reflects the concerted effort taken by the University of North Carolina, Wilmington (UNCW) team led by W. McLellan to boost the taxonomic precision of beaked whale sightings in this area, which they heavily surveyed (McLellan et al. 2018). Despite being a climatological model there was some seasonal variation predicted, with the lowest abundance (2,234) predicted in May and the highest abundance predicted in August (6,984) (Figure 32, Table 13).

The extrapolation statistics show some extrapolation in univariate space. Depth showed a few cells of extrapolated values at the eastern mid-Atlantic edge of the study area (Figure 29). The distance to cyclonic eddy covariate showed some isolated instances of univariate extrapolation in January through May and July through September in the eastern edge of the mid-Atlantic and southern portions of the study area (Figure 30). In this case distances “inside” the eddy ring are negative values, and the extrapolation cells indicate very large eddies, with large cores that are far from the ring in the negative direction. This is unlikely to be a major issue, as large eddies needed to trigger the extrapolation were infrequent and as such, unlikely to have yielded a big effect in the final model.

In comparison to the SAR, the year-round mean abundance for the NEFSC region (2,010) was 46% lower than the SAR estimate (3,755). In the SEFSC region, the new model estimated 77% lower abundance (645) compared to the SAR estimate (2,812). This resulted in a combined year-round mean estimate (2,655) that was 60% lower than the SAR estimate (6,567). We recognize that these estimates are low compared to the SAR, perhaps due to differences in $g(0)$ estimation and detection functions, or something particular to the 2016 survey year from which the SAR estimates were generated.

In comparison to the Roberts et al. (2017) model (3,085) the new model predicts 29% more animals (4346), but similarly, highest abundance was predicted in the northern region for both models.

References

- Baird RW, McSweeney DJ, Ligon AD, Webster DL (2004) Tagging Feasibility and Diving of Cuvier's Beaked Whales (*Ziphius cavirostris*) and Blainville's Beaked Whales (*Mesoplodon densirostris*) in Hawai'i.
- Barco SG, Burt L, DePerte A, Digiovanni R Jr. (2015) Marine Mammal and Sea Turtle Sightings in the Vicinity of the Maryland Wind Energy Area July 2013-June 2015, VAQF Scientific Report #2015-06. Virginia Aquarium & Marine Science Center Foundation, Virginia Beach, VA
- Barlow J (1999) Trackline detection probability for long-diving whales. In: Marine Mammal Survey and Assessment Methods. Balkema, Rotterdam, The Netherlands, pp 209–221
- Baumgartner MF (1997) The Distribution of Risso's Dolphin (*grampus Griseus*) with Respect to the Physiography of the Northern Gulf of Mexico. *Marine Mammal Science* 13:614–638. doi: [10.1111/j.1748-7692.1997.tb00087.x](https://doi.org/10.1111/j.1748-7692.1997.tb00087.x)
- Becker JJ, Sandwell DT, Smith WHF, Braud J, Binder B, Depner J, Fabre D, Factor J, Ingalls S, Kim S-H, Ladner R, Marks K, Nelson S, Pharaoh A, Trimmer R, Von Rosenberg J, Wallace G, Weatherall P (2009) Global Bathymetry and Elevation Data at 30 Arc Seconds Resolution: SRTM30_PLUS. *Marine Geodesy* 32:355–371. doi: [10.1080/01490410903297766](https://doi.org/10.1080/01490410903297766)
- Buckland ST, Anderson DR, Burnham KP, Laake JL, Borchers DL, Thomas L (2001) Introduction to Distance Sampling: Estimating Abundance of Biological Populations. Oxford University Press, Oxford, UK
- Burt ML, Borchers DL, Jenkins KJ, Marques TA (2014) Using mark-recapture distance sampling methods on line transect surveys. *Methods in Ecology and Evolution* 5:1180–1191. doi: [10.1111/2041-210X.12294](https://doi.org/10.1111/2041-210X.12294)
- Chelton DB, Schlax MG, Samelson RM (2011) Global observations of nonlinear mesoscale eddies. *Progress in Oceanography* 91:167–216. doi: [10.1016/j.pocean.2011.01.002](https://doi.org/10.1016/j.pocean.2011.01.002)
- Cole T, Gerrior P, Merrick RL (2007) [Methodologies of the NOAA National Marine Fisheries Service Aerial Survey Program for Right Whales \(*Eubalaena glacialis*\) in the Northeast U.S., 1998-2006](#). U.S. Department of Commerce, Woods Hole, MA
- Cotter MP (2019) Aerial Surveys for Protected Marine Species in the Norfolk Canyon Region: 2018–2019 Final Report. HDR, Inc., Virginia Beach, VA
- Foley HJ, Paxton CGM, McAlarney RJ, Pabst DA, Read AJ (2019) Occurrence, Distribution, and Density of Protected Species in the Jacksonville, Florida, Atlantic Fleet Training and Testing (AFTT) Study Area. Duke University Marine Lab, Beaufort, NC
- Garrison LP (2020) [Abundance of cetaceans along the southeast U.S. East coast from a summer 2016 vessel survey. PRD Contribution # PRD-2020-04](#). NOAA National Marine Fisheries Service, Southeast Fisheries Science Center, Miami, FL
- Hayes SA, Josephson E, Maze-Foley K, Rosel PE, Byrd B, Chavez-Rosales S, Cole TV, Garrison LP, Hatch J, Henry A, Horstman SC, Litz J, Lyssikatos MC, Mullin KD, Orphanides C, Pace RM, Palka DL, Powell J, Wenzel FW (2020) [US Atlantic and Gulf of Mexico Marine Mammal Stock Assessments - 2019](#). NOAA National Marine Fisheries Service, Northeast Fisheries Science Center, Woods Hole, MA
- Laake JL, Calambokidis J, Osmek SD, Rugh DJ (1997) Probability of Detecting Harbor Porpoise From Aerial Surveys: Estimating $g(0)$. *Journal of Wildlife Management* 61:63–75. doi: [10.2307/3802415](https://doi.org/10.2307/3802415)
- Lehodey P, Senina I, Murtugudde R (2008) A spatial ecosystem and populations dynamics model (SEAPODYM)—Modeling of tuna and tuna-like populations. *Progress in Oceanography* 78:304–318. doi: [10.1016/j.pocean.2008.06.004](https://doi.org/10.1016/j.pocean.2008.06.004)
- Leiter S, Stone K, Thompson J, Accardo C, Wikgren B, Zani M, Cole T, Kenney R, Mayo C, Kraus S (2017) North Atlantic right whale *Eubalaena glacialis* occurrence in offshore wind energy areas near Massachusetts and Rhode Island, USA. *Endang Species Res* 34:45–59. doi: [10.3354/esr00827](https://doi.org/10.3354/esr00827)
- MacLeod CD, Perrin WF, Pitman R, Barlow J, Ballance L, D Amico A, Gerrodette T, Joyce G, Mullin KD, Palka DL, others (2005) [Known and inferred distributions of beaked whale species \(Cetacea: Ziphiidae\)](#). *Journal of Cetacean Research and Management* 7:271.
- Mallette SD, Lockhart GG, McAlarney RJ, Cummings EW, McLellan WA, Pabst DA, Barco SG (2014) Documenting Whale Migration off Virginia's Coast for Use in Marine Spatial Planning: Aerial and Vessel Surveys in the Proximity of the Virginia Wind Energy Area (VA WEA), VAQF Scientific Report 2014-08. Virginia Aquarium & Marine Science Center Foundation, Virginia Beach, VA
- Mallette SD, Lockhart GG, McAlarney RJ, Cummings EW, McLellan WA, Pabst DA, Barco SG (2015) Documenting Whale Migration off Virginia's Coast for Use in Marine Spatial Planning: Aerial Surveys in the Proximity of the Virginia Wind

- Energy Area (VA WEA) Survey/Reporting Period: May 2014 - December 2014, VAQF Scientific Report 2015-02. Virginia Aquarium & Marine Science Center Foundation, Virginia Beach, VA
- Mallette SD, McAlarney RJ, Lockhart GG, Cummings EW, Pabst DA, McLellan WA, Barco SG (2017) [Aerial Survey Baseline Monitoring in the Continental Shelf Region of the VACAPES OPAREA: 2016 Annual Progress Report](#). Virginia Aquarium & Marine Science Center Foundation, Virginia Beach, VA
- Marsh H, Sinclair DF (1989) Correcting for Visibility Bias in Strip Transect Aerial Surveys of Aquatic Fauna. *The Journal of Wildlife Management* 53:1017. doi: [10.2307/3809604](#)
- McAlarney R, Cummings E, McLellan W, Pabst A (2018) Aerial Surveys for Protected Marine Species in the Norfolk Canyon Region: 2017 Annual Progress Report. University of North Carolina Wilmington, Wilmington, NC
- McLellan WA, McAlarney RJ, Cummings EW, Read AJ, Paxton CGM, Bell JT, Pabst DA (2018) Distribution and abundance of beaked whales (Family Ziphiidae) Off Cape Hatteras, North Carolina, U.S.A. *Marine Mammal Science*. doi: [10.1111/mms.12500](#)
- Mesgaran MB, Cousens RD, Webber BL (2014) Here be dragons: A tool for quantifying novelty due to covariate range and correlation change when projecting species distribution models. *Diversity Distrib* 20:1147–1159. doi: [10.1111/ddi.12209](#)
- Miller DL, Becker EA, Forney KA, Roberts JJ, Cañadas A, Schick RS (2022) Estimating uncertainty in density surface models. *PeerJ* 10:e13950. doi: [10.7717/peerj.13950](#)
- Moulins A, Rosso M, Nani B, Würtz M (2007) Aspects of the distribution of Cuvier’s beaked whale (*Ziphius Cavirostris*) in relation to topographic features in the *Pelagos Sanctuary* (north-western Mediterranean Sea). *J Mar Biol Ass* 87:177–186. doi: [10.1017/S0025315407055002](#)
- O’Brien O, Pendleton DE, Ganley LC, McKenna KR, Kenney RD, Quintana-Rizzo E, Mayo CA, Kraus SD, Redfern JV (2022) Repatriation of a historical North Atlantic right whale habitat during an era of rapid climate change. *Sci Rep* 12:12407. doi: [10.1038/s41598-022-16200-8](#)
- Palka D (2020) [Cetacean Abundance in the US Northwestern Atlantic Ocean Summer 2016](#). [Northeast Fish Sci Cent Ref Doc. 20-05](#). NOAA National Marine Fisheries Service, Northeast Fisheries Science Center, Woods Hole, MA
- Palka D, Aichinger Dias L, Broughton E, Chavez-Rosales S, Cholewiak D, Davis G, DeAngelis A, Garrison L, Haas H, Hatch J, Hyde K, Jech M, Josephson E, Mueller-Brennan L, Orphanides C, Pegg N, Sasso C, Sigourney D, Soldevilla M, Walsh H (2021) [Atlantic Marine Assessment Program for Protected Species: FY15 – FY19 \(OCS Study BOEM 2021-051\)](#). U.S. Department of the Interior, Bureau of Ocean Energy Management, Washington, DC
- Palka DL (2006) [Summer abundance estimates of cetaceans in US North Atlantic navy operating areas \(NEFSC Reference Document 06-03\)](#). U.S. Department of Commerce, Northeast Fisheries Science Center, Woods Hole, MA
- Palka DL, Chavez-Rosales S, Josephson E, Cholewiak D, Haas HL, Garrison L, Jones M, Sigourney D, Waring G, Jech M, Broughton E, Soldevilla M, Davis G, DeAngelis A, Sasso CR, Winton MV, Smolowitz RJ, Fay G, LaBrecque E, Leiness JB, Dettloff K, Warden M, Murray K, Orphanides C (2017) [Atlantic Marine Assessment Program for Protected Species: 2010-2014 \(OCS Study BOEM 2017-071\)](#). U.S. Department of the Interior, Bureau of Ocean Energy Management, Washington, DC
- Quintana-Rizzo E, Leiter S, Cole T, Hagbloom M, Knowlton A, Nagelkirk P, O’Brien O, Khan C, Henry A, Duley P, Crowe L, Mayo C, Kraus S (2021) Residency, demographics, and movement patterns of North Atlantic right whales *Eubalaena glacialis* in an offshore wind energy development area in southern New England, USA. *Endang Species Res* 45:251–268. doi: [10.3354/esr01137](#)
- Read AJ, Barco S, Bell J, Borchers DL, Burt ML, Cummings EW, Dunn J, Fougères EM, Hazen L, Hodge LEW, Laura A-M, McAlarney RJ, Peter N, Pabst DA, Paxton CGM, Schneider SZ, Urian KW, Waples DM, McLellan WA (2014) [Occurrence, distribution and abundance of cetaceans in Onslow Bay, North Carolina, USA](#). *Journal of Cetacean Research and Management* 14:23–35.
- Redfern JV, Krynka KA, Weiss L, Hodge BC, O’Brien O, Kraus SD, Quintana-Rizzo E, Auster PJ (2021) Opening a Marine Monument to Commercial Fishing Compromises Species Protections. *Front Mar Sci* 8:645314. doi: [10.3389/fmars.2021.645314](#)
- Roberts JJ, Best BD, Dunn DC, Treml EA, Halpin PN (2010) Marine Geospatial Ecology Tools: An integrated framework for ecological geoprocessing with ArcGIS, Python, R, MATLAB, and C++. *Environmental Modelling & Software* 25:1197–1207. doi: [10.1016/j.envsoft.2010.03.029](#)
- Roberts JJ, Best BD, Mannocci L, Fujioka E, Halpin PN, Palka DL, Garrison LP, Mullin KD, Cole TVN, Khan CB, McLellan WA, Pabst DA, Lockhart GG (2016) Habitat-based cetacean density models for the U.S. Atlantic and Gulf of Mexico. *Scientific Reports* 6:22615. doi: [10.1038/srep22615](#)

- Roberts JJ, Mannocci L, Halpin PN (2017) Final Project Report: Marine Species Density Data Gap Assessments and Update for the AFTT Study Area, 2016-2017 (Opt. Year 1), Document Version 1.4. Duke University Marine Geospatial Ecology Lab, Durham, NC
- Roberts JJ, Yack TM, Halpin PN (2023) Marine mammal density models for the U.S. Navy Atlantic Fleet Training and Testing (AFTT) study area for the Phase IV Navy Marine Species Density Database (NMSDD), Document Version 1.3. Duke University Marine Geospatial Ecology Lab, Durham, NC
- Robertson FC, Koski WR, Brandon JR, Thomas TA, Trites AW (2015) [Correction factors account for the availability of bowhead whales exposed to seismic operations in the Beaufort Sea.](#) *Journal of Cetacean Research and Management* 15:35–44.
- Schlax MG, Chelton DB (2016) [The "Growing Method" of Eddy Identification and Tracking in Two and Three Dimensions.](#) College of Earth, Ocean and Atmospheric Sciences, Oregon State University, Corvallis, OR
- Stone KM, Leiter SM, Kenney RD, Wikgren BC, Thompson JL, Taylor JKD, Kraus SD (2017) Distribution and abundance of cetaceans in a wind energy development area offshore of Massachusetts and Rhode Island. *J Coast Conserv* 21:527–543. doi: [10.1007/s11852-017-0526-4](#)
- Waring GT, Hamazaki T, Sheehan D, Wood G, Baker S (2001) [Characterization of beaked whale \(Ziphiidae\) and sperm whale \(Physeter macrocephalus\) summer habitat in shelf-edge and deeper waters off the northeast US.](#) *Marine Mammal Science* 17:703–717.
- Zoidis AM, Lomac-MacNair KS, Ireland DS, Rickard ME, McKown KA, Schlesinger MD (2021) Distribution and density of six large whale species in the New York Bight from monthly aerial surveys 2017 to 2020. *Continental Shelf Research* 230:104572. doi: [10.1016/j.csr.2021.104572](#)